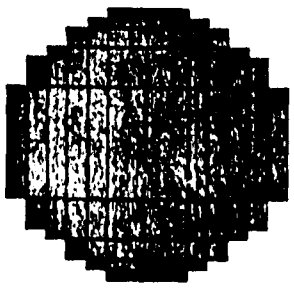


AD-A152 728

CONVERGENCE RATE IN ADAPTIVE RADAR  
TSC-PD-137-4  
John D. Mallett  
Irving S. Keed  
Frank P. Hopper  
February 1976

DTIC FILE COPY



DTIC  
ELECTE  
APR 24 1985  
S D

APPROVED FOR PUBLIC RELEASE  
DISTRIBUTION UNLIMITED

Technology Service Corporation

85 4 23 07

CONVERGENCE RATE IN ADAPTIVE RADAR

TSC-PD-137-4

John D. Mallett  
Irving S. Keed  
Frank P. Hopper

February 1976

Fourth Quarterly Report

Submitted to:  
THE NAVAL AIR SYSTEMS COMMAND  
on  
Contract N00019-75-C-0128

Accession For	
NTIS GRA&I	<input checked="" type="checkbox"/>
DTIC TAB	<input type="checkbox"/>
Unannounced	<input type="checkbox"/>
Justification	
By _____	
Distribution/ _____	
Availability Codes	
Dist	Avail and/or Special
A-1	



APPROVED FOR PUBLIC RELEASE:  
DISTRIBUTION UNLIMITED

TABLE OF CONTENTS

<u>Section</u>	<u>Page</u>
1.0 INTRODUCTION . . . . .	1
2.0 SIMULATION OF QUANTIZATION AND LIMITING. . . . .	2
2.1 QUANTIZATION. . . . .	9
2.2 LIMITING. . . . .	12
2.3 LIMITING AND QUANTIZATION . . . . .	15
3.0 SOME CONVERGENCE EXPERIMENTS . . . . .	24
REFERENCES . . . . .	35
APPENDIX I . . . . .	36
APPENDIX II. . . . .	54

## 1.0 INTRODUCTION

This is the fourth and final quarterly progress report for a one year study of convergence in adaptive radar. During a series of earlier adaptive radar studies<sup>[1,2]</sup> at TSC, funded by Naval Air Systems Command, a method of optimizing both the angular and doppler response in AMTI (airborne moving target indication radars) was described, analyzed, and simulated in some detail. These studies showed that adaptive AMTI radar can provide a major improvement in performance in a mixed clutter/ECM environment.

In the first progress report<sup>[3]</sup> the basic adaptive AMTI technique was described, and three adaptive algorithms were compared. These algorithms were sample matrix inversion SMI, inverse matrix update IMU, and the Applebaum loop algorithm. Both SMI and IMU algorithms are shown to be very fast in terms of number of data samples required for convergence. These algorithms are more complicated than the loop technique, though, and are probably best implemented using digital techniques. Section 2 of this report presents results of a computer simulation of analogue to digital (A/D) conversion. A theory predicting the performance loss due to quantization was presented in progress report 3 of this contract and is included as Appendix I. This theory is compared with simulation results in Section 2. The program used to obtain the results of Section 2 is included as Appendix II. In Section 3 of this report some further results are shown for the IMU technique, using the program listed in reference 3.

## 2.0 SIMULATION OF QUANTIZATION AND LIMITING

In this section we consider the effect of converting the input analogue data to digital data in an adaptive AMTI array, including the ability to reject clutter. A/D conversion introduces two different types of non linearity, one is quantization which produces a step like approximation to a straight line transfer function and the other is limiting which renders the output constant after a particular input level is reached. These effects are important, since the number of bits used in a quantizer is limited for economic reasons and must be as small as is consistent with good performance. The above nonlinearities are simulated separately and together using the computer programs in Appendix II. The simulation of quantization and limiting separately allows comparison with the theoretical results for quantization noise given in Appendix I.

The example considered for simulation is an AMTI radar system in which the weights  $W_{ep}$  are multiplied by the output of a number  $E$  of receiving antenna elements on each of a number  $F$  of pulses and then added to obtain the radar output. The non linearities are introduced as shown in Figure 2.1. The weights as in earlier studies can be nearly optimized, using data samples collected by the radar. A single sample of data is defined as the set of returns from a single range bin at each element on each pulse, so that for a 2 pulse MTI with 4 antenna elements, a sample would contain eight complex values. All weights and voltages are complex thereby preserving both phase and

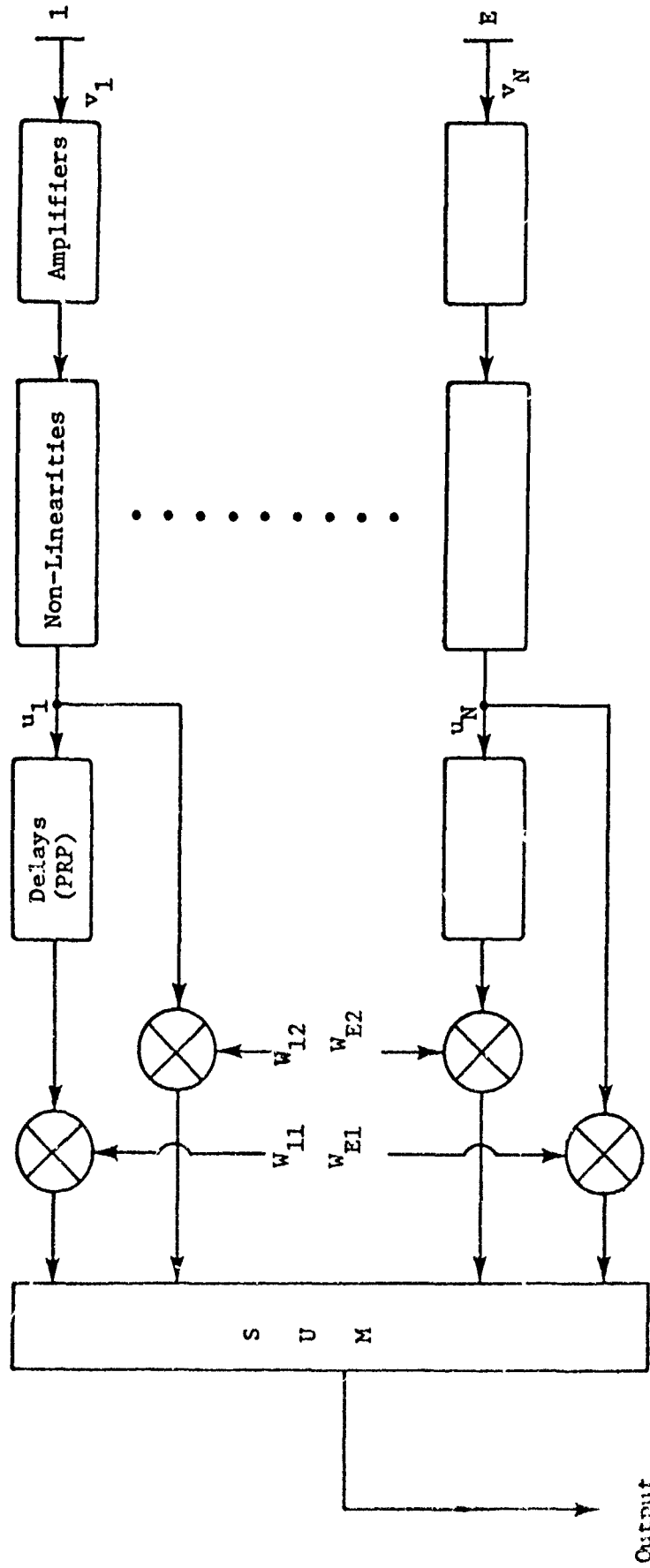


Figure 2.1. Functional Diagram of Adaptive Radar With Non-Linearities.

amplitude information. Each channel shown in Figure 2.1 consists, in fact, of two quadrature channels, one in-phase I, the other 90° out-of-phase Q. On transmission the elements are combined with equal weighting to form a fixed transmit beam.

In a computer simulation where the interference or noise (in this case distributed ground clutter and receiver noise) is known exactly, an ideal covariance matrix  $M$  for a linear system is computed as

$$M_{mn} = \sum_{j=1}^J V_{m_j}^* V_{n_j} \exp \left( \frac{2\pi i}{\lambda} (D_{n_j} - D_{m_j}) \right) \quad (2-1)$$

where

$V_{m_j}$  = the voltage at the  $m^{\text{th}}$  element (pulse) from the  $j^{\text{th}}$  scatterer

$D_{m_j}$  = distance from scatterer to element

$\lambda$  = transmitter wavelength

\* means complex conjugate

For convenience the indexing over antenna elements and pulses is combined so that  $V_{ep}$  becomes  $V_m$  where  $m = e + (p-1)E$ . Included in  $V$  is the scatterer amplitude and any other amplitude weighting such as the transmitter antenna pattern and individual element patterns.

The signal-to-clutter or MTI gain is given in vector notation by

$$G = \frac{|WS|^2}{WMM^*} \cdot \frac{1}{(S/C)_0} \quad (2-2)$$

for a set of weights  $W$ , where  $(S/C)_o$  is the signal to clutter obtained on a single pulse with uniform weighting on receive and transmit. This factor is used for normalization.

As explained in previous references<sup>[1-4]</sup> the weights that maximize  $S/C$  or  $G$  are known to be

$$W_o = M^{-1}S^* \quad (2-3)$$

and

$$G_m = \frac{|W_o S|^2}{W_o M W_o^*} \frac{1}{(S/C)_o} = S M^{-1} S^* \frac{1}{(S/C)_o} \quad (2-4)$$

where  $S$  is the desired signal vector. When non-linearities are present, for example as indicated in Figure 2.1, the clutter covariance matrix cannot always be readily calculated. Instead it can be found by using computer generated data samples to form a sample covariance matrix (or its inverse) as it would be done in an adaptive radar using digital processing. The sample covariance matrix  $\hat{M}$  is given by

$$\hat{M}_{mn} = \frac{1}{S} \sum_{j=1}^S U_{mj}^* U_{nj} \quad (2-5)$$

where the summation is over independent samples  $S$ . The  $U_{mj}$ 's are the element voltages after the non-linearities are applied. In the computer simulation, each voltage for a given sample is generated by choosing a different set of Gaussian distributed random numbers for a prescribed set of scatterers. The sample covariance matrix is an approximation to the ideal matrix for a set of scatterers. As it was shown previously<sup>[5]</sup>, the convergence is very fast.

The sample covariance matrix can be used to compute a set of weights.

Thus

$$W_s = \hat{M}^{-1} S^* \quad (2-6)$$

The question then is how to test the weights  $W_s$  generated from a sample covariance matrix. It is meaningful with a linear system to test the  $W_s$  using the ideal covariance matrix since  $\hat{M} \rightarrow M$  as the number of samples becomes large. With non-linearities present this is not so.

Two cases are of practical interest. In case 1 a sample matrix is found  $\hat{M}_1$  and used to create optimum weights  $W_1$  for  $\hat{M}_1$ . Then these weights are tested on the same sample data used to obtain the weights. Thus Case 1

$$W_1 = \hat{M}_1^{-1} S^* \quad (2-7)$$

$$G_1 = \left( \frac{W_1 \hat{M}_1 W_1^*}{W_1 \hat{M}_1 W_1^*} - 1 \right) \frac{1}{(S/C)_0} \approx \frac{|W_1 S|^2}{W_1 \hat{M}_1 W_1^*} \frac{1}{(S/C)_0} \quad (2-8)$$

where  $\hat{M}_{1s}$  and  $\hat{M}_1$  are the covariance matrices with and without signal.

Case 2 is similar to the above except that the sample matrix used for testing the weights  $W_1$  is made up of different samples. Thus in Case 2

$$W_1 = \hat{M}_1^{-1} S^* \quad (2-9)$$

$$G_2 \approx \frac{|W_1 S|^2}{W_1 \hat{M}_2 W_1^*} \frac{1}{(S/C)_0} \quad (2-10)$$

In this formulation the signal is not present in the simulation and is assumed to be unaffected by the non-linearities. Since signal loss is quite small even with hard limiting this is a reasonable approximation.

Case 2 is easier to apply in practice. For Case 1 to be implemented, the data from all elements is stored and used to form a covariance matrix, then the weights derived are used on each range cell individually. This requires more storage than in Case 2, where the weights are used on succeeding range bins as the data arrives.

In practice the weights would be applied to each range bin individually to maximize the signal-to-clutter gain. For simulation purposes one is interested not in individual, but in average performance, therefore one can apply the weights to the already summed covariance matrices  $\hat{M}_1$  or  $\hat{M}_2$  as in Equation 2.8 or 2.10. This is equivalent to applying the weight to each sample individually and averaging the results.

The relations discussed so far contain the assumption that the signal is not present during the collection of data, i.e. that no signal is present in the covariance matrix used to determine the optimum weights. This situation cannot be strictly true in Case 1, or no signals would be detected. It could be true in Case 2, if the data used for determining the weights were obtained over a region known to contain no signals. From previous simulations<sup>[5]</sup> it has been found that little degradation in performance occurs when signals are present. If signals are small the dominance of clutter which is present in many range bins compared to the one or two for signals determines the weights as if the signals were not present. If the signal is large detection is not a problem anyway, so that Case 1 as well as Case 2 apply to realizable cases.

Two types of non-linearities are explored in the simulation, quantization which occurs in the conversion of analog data to digital as indicated in Figure 2.2, where a linear function is replaced by a

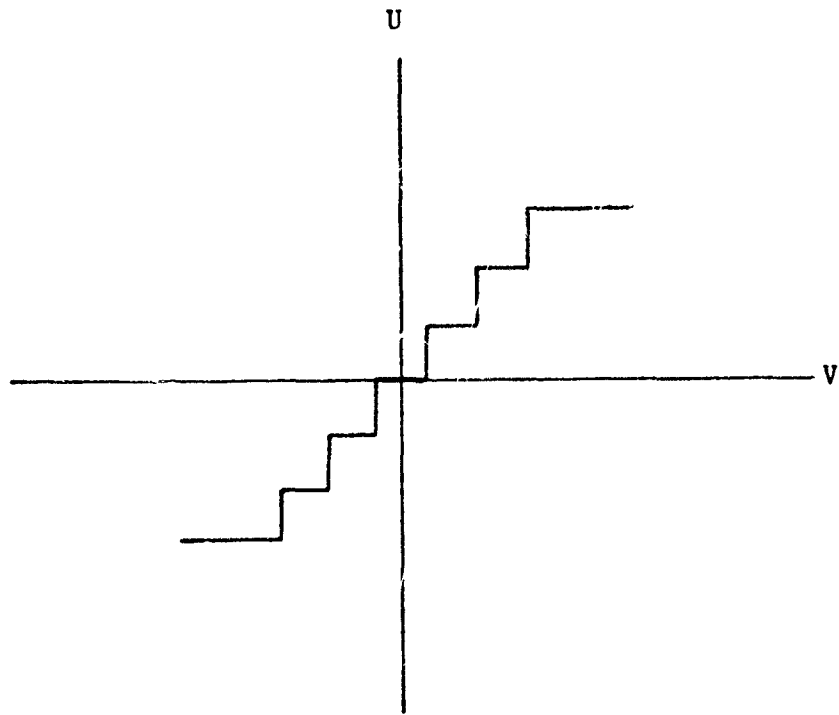


Figure 2.2. A/D Converter With Equal Step Sizes.

stair step, and limiting as also indicated in Figure 2.2. The limiting can be either in the I and Q channels in which case phase distortion occurs, or amplitude (envelope) limiting as might be performed at IF before the quadrature channels are determined. In the latter case the amplitude is limited without causing phase distortion.

### 2.1 QUANTIZATION

In Table 2.1 are shown results for quantization noise with no limiting for various values of step size  $\Delta$  divided by RMS input voltage  $\sigma$ . The example used consists of a 4 element antenna with  $.5\lambda$  spacing between elements and 2 pulse MTI. The beam is broadside to the array and is aimed in the direction of travel of the radar which is moving at a rate of  $.2\lambda$  per pulse. Thirty scatterers are distributed uniformly over  $180^\circ$  to simulate ground clutter. Under these conditions the ideal MTI gain as defined earlier is 53.8 dB.

The losses shown are the MTI gain values obtained with quantization divided by the ideal performance and expressed in dB. In this Table 24 or  $3N^{[1]}$  samples are used to form the sample covariance matrix  $\hat{M}_1$  which is used to generate the weights  $W_1$ . These weights are then tested on  $\hat{M}_1$  for Case 1 and on  $\hat{M}_2$  which is formed from an equal number but different set of samples. The experiment is repeated 12 times in this Table, i.e. 12 runs and the results of the runs are averaged. The variance as shown is quite small.

Some of the simulation values shown for Case 1 are negative indicating

[1] Where N is the number of degrees of freedom which in this case is  $2 \times 4 = 8$ .

Table 2.1

QUANTIZATION LOSS (dB) (NO LIMITING)

2 pulse MTI 4 elements                      30 clutter scatterers uniformly distributed over 180°

Platform motion  $0.2\lambda$  per pulse              Beam angle  $0^\circ$  from velocity vector

Ideal performance (no quantization)       $G = 53.8$  dB

Samples used in  $\hat{M} = 24$  (3N)              Runs averaged = 12

Theoretical Quant. Loss =  $L_Q, L_Q'$               Theoretical Sample Loss  $L_S = 1.43$  dB

$\Delta/\sigma$	Case	$L_Q$	$L_Q'$	$L_Q + L_S$	Simulation Loss	Variance
0	1				-1.65	.034
	2	0	0	1.4	1.24	.021
.01	1				.02	.073
	2	1.90	3.47	3.33	2.97	.042
.02	1				3.44	.056
	2	5.05		6.48	6.586	.038
.04	1				7.873	.075
	2	9.91		11.33	10.94	.126
.08	1				13.65	.059
	2	15.54		16.98	16.63	.060

Case 1- $W_1$  tested on  $\hat{M}_1$  Case 2  $W_1$  tested on  $\hat{M}_2$ . All values are in dB (-) indicates a gain.  $\Delta/\sigma$  = step size/RMS voltage.

an improvement over the so called ideal linear case. This is possible when the weights generated from a particular set of samples are used on the same set as in Case 1. The same weights give poorer results when used on other sets of data generated by the same process.

Two theoretical results have been developed for loss from ideal performance. One loss is due to finite sample size and is given by<sup>[5]</sup>

$$L_s = 10. \log_{10} \left( \frac{S+2-N}{S+1} \right) \quad (2-11)$$

where S is the number of samples used, and N is the degrees of freedom, i.e. E · P in this case.

The other loss due to quantization was derived in Progress Report #3 and is reproduced in Appendix 1. This is given by

$$L_Q = 10. \text{Log}_{10} \frac{S^* M^{-1} S}{S^* M^{-1} Q} \quad (2-12)$$

where

$$M_Q = M + \frac{\Delta^2}{6} I \quad (2-13)$$

Using another approximation, a second formula for the loss was obtained as

$$L_Q = 10. \text{Log}_{10} \left( 1 - \frac{\Delta^2}{6} \frac{W^* W}{S^* M^{-1} S} \right) \quad (2-14)$$

In Table 2.1 the simulation and theoretical losses are shown. It is seen that there is good agreement between Case 2 simulation results and the total losses based on sample size and quantization loss. The approximate results for  $L_Q$  loss do not give such good agreement.

Table 2.2 shows the losses for various numbers of samples in the covariance matrices. Theoretical and simulation results are in very good agreement and the variance seems reasonable for the values chosen.

## 2.2 LIMITING

In this section limiting without quantization is explored by simulation. Two kinds of limiting are considered. Amplitude or envelope in which the vector amplitude is limited but phase is not distorted, and limiting in the IQ channels where both phase and amplitude are affected. These two types are illustrated in Figure 2.3.

While there are theoretical results for hard limiting, it is difficult to obtain theoretical results for linear operation with the various degrees of soft limiting used in this case. Simulation results are shown in Table 2.3 for limiting in the IQ channels and in envelope, as a function of limit levels divided by RMS input voltage  $\sigma$ .

It is interesting to note that for strong limiting (small values of  $S/\sigma$ ), IQ limiting seems to produce the greater loss. This perhaps is due to the greater phase distortion. At values of  $S/\sigma$  producing less limiting, losses seem to be higher when amplitude limiting is used. Also, the variance is quite high for the lower limiting values. Both of these results may be due to the fact that for larger values of  $S/\sigma$  there is less limiting in IQ, thereby causing less chance of a degraded

Table 2.2

QUANTIZATION LOSS (dB) (NO LIMITING)

2 pulse MTI 4 elements

30 clutter scatterers uniformly  
distributed over 180°

Platform motion 0.2λ per pulse

Beam angle 0° from velocity vector

Ideal performance (no quantization) S/C - 53.8 dB

Samples used in  $\hat{M} = 24$  (3N)

Runs averaged = 12

Theoretical Quant. Loss =  $L_Q, L_Q'$ Theoretical Sample Loss  $L_S$ 

$\Delta/\sigma$	Case	$L_Q$	$L_Q'$	Sample=64 (8N) Runs=4 $L_S=.5$ dB			Sample=32 (4N) Runs=9 $L_S=1.03$ dB			Sample=16 (2N) Runs=19 $L_S=2.3$ dB		
				$L_Q+L_S$	Sim. Loss	Var.	$L_Q+L_S$	Sim. Loss	Var.	$L_Q+L_S$	Sim. Loss	Var.
.001	1			-.61		.007	-1.275		.015	-3.02		.068
	2	.024	.024	.52	.33	.001	1.06	.923	.026	2.33	2.35	.073
.01	1				1.22	.03		.55	.025		-1.1	.121
	2	1.91		2.4	2.3	.015	2.94	2.7	.035	4.2	4.01	.094
-1	1				16.9	.007		16.13	.047		14.35	.273
	2	17.42		17.9	18.02	.012	18.46	18.4	.028	19.72	19.37	.102

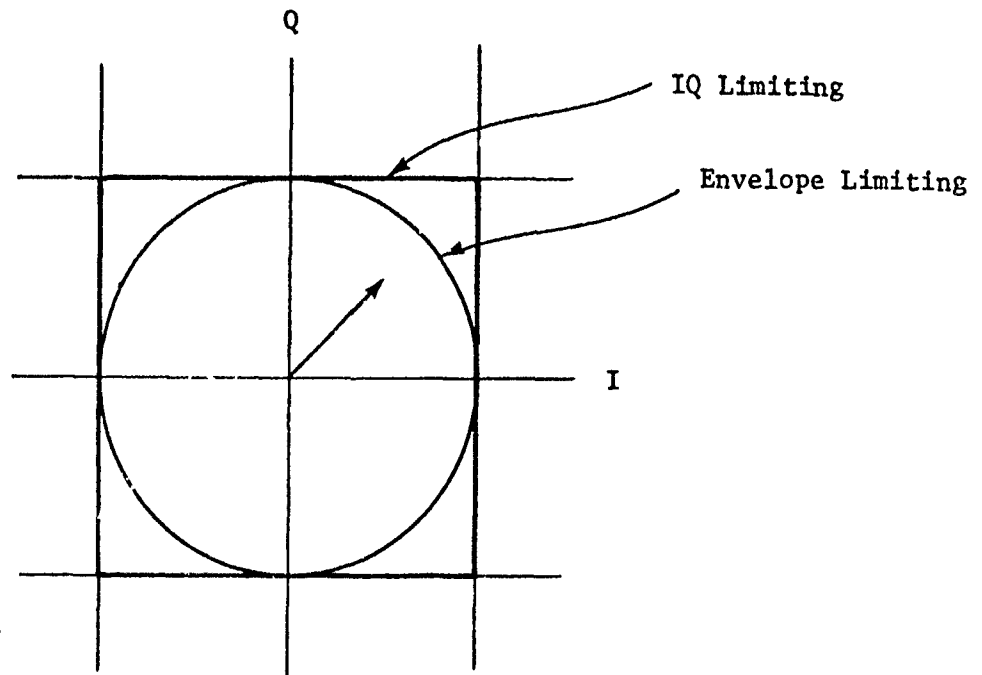


Figure 2.3. Showing IQ and Complex Envelope Limiting.

result. When limiting does occur considerable degradation results. This is usually indicated by drastically increased variance.

The percent limiting, shown in Table 2.3, is obtained by counting the number of times that limiting occurs during simulation. The reason that there is more limiting in the envelope case (the circle in Figure 2.3) is probably that the sample vectors have more "non-limit" area in the complex plan when IQ limiting is used (the square in Figure 2.3).

### 2.3 LIMITING AND QUANTIZATION

Simulator MTI gains are shown in Figure 2.4 and 2.5 for quantization and limiting combined as a function of normalized saturation level  $S/\sigma$  ( $\sigma$  = RMS input voltage). The results are shown for 8, 9 and 10 bits. As  $S/\sigma$  increases, limiting decreases but the quantization step size  $\Delta$  increases so that there are optimum values of  $S/\sigma$ . Since quantization noise degrades performance slowly compared to limiting, there is a fairly broad region of  $S/\sigma$  values over which to operate.

There is little difference as indicated by Figure 2.4 and 2.5 between IQ and envelope limiting in the region of small limiting as might be expected. With strong limiting envelope limiting shows better but highly degraded performance.

In Figures 2.6 and 2.7 results are shown for a case with higher MTI gain. In this case the scan angle is  $90^\circ$  to the flight path, and the interpulse motion is close to  $\lambda/4$ , the velocity and angle for which perfect platform motion compensation is possible. MTI gain is plotted in this section rather than losses to illustrate performance at different gain levels. The Case 1 performance in which  $W_1$  is used with  $\hat{M}_1$  rather than  $\hat{M}_2$  (Case 2), exceeds the steady state or ideal performance. This

Table 2.3

## Simulation Results for Limiting Only

2 pulse MTI      4 elements      30 scatters

Platform motion =  $0.2\lambda$ /pulse      Beam angle 0.0

Ideal G = 53.8 dB

Sample = 64 (8N)      Runs = 4

S/ $\sigma$	Case	I and Q			Envelope		
		Loss(dB)	Variance	% Limiting	Loss(dB)	Variance	% Limiting
1.5	1	30.5	.015	27	21.3	.039	32
	2	31.7	.001		22.4	.014	
2.0	1	24.0	.07	9	18.4	.056	14
	2	26.7	.17		20.6	.015	
2.5	1	12.3	.533	2.66	12.2	.162	4.33
	2	15.9	1.25		16.1	.023	
3.0	1	2.34	.646	.39	2.91	.82	.86
	2	4.63	.859		5.74	.92	
3.5	1	.632	.01	.04	.009	.157	.23
	2	.28	.002		1.4	.128	

S/ $\sigma$  = Saturation level/RMS voltage.

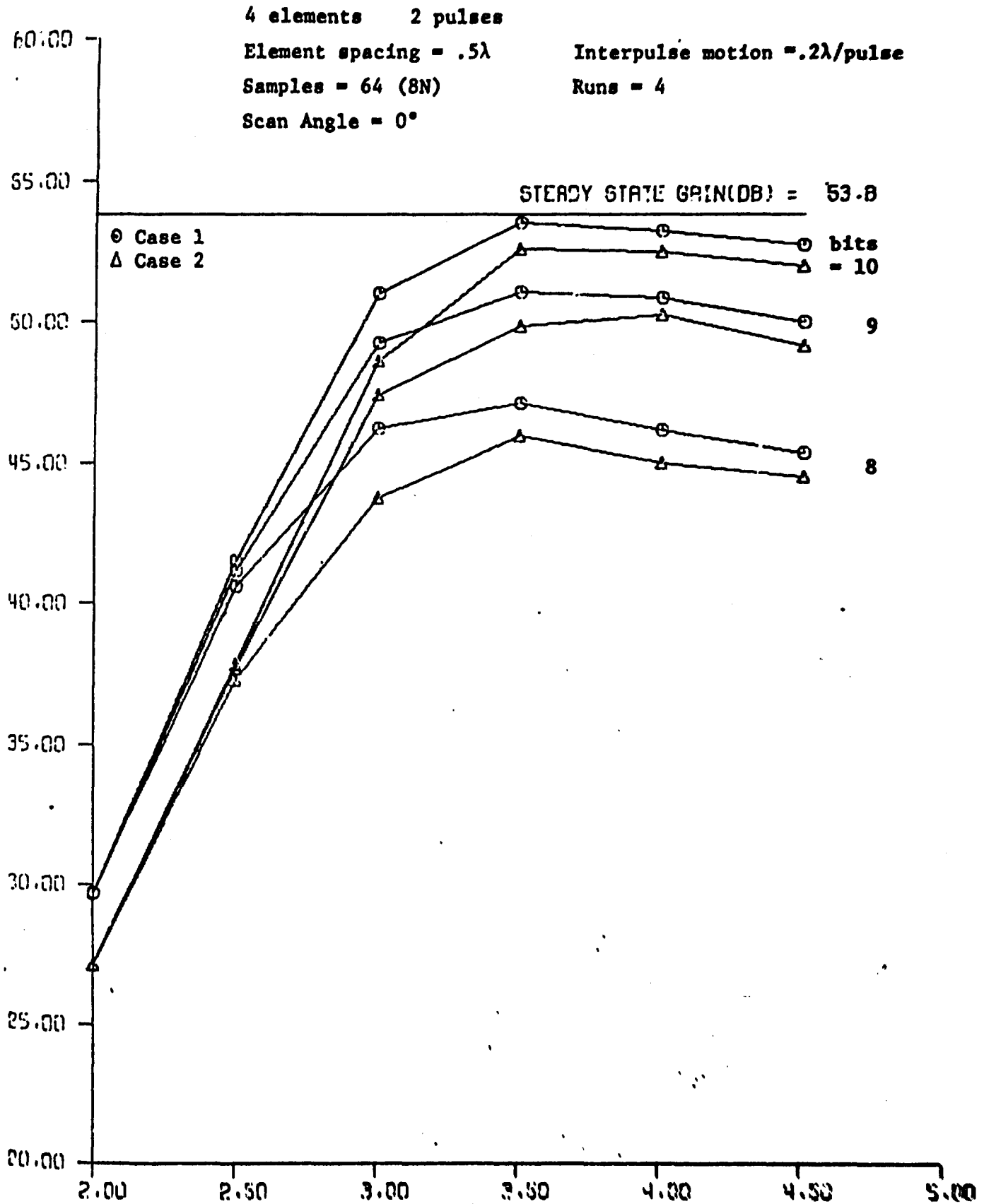


Figure 2.4 MTI Gain vs IQ Limit Level and Number of Bits

4 elements 2 pulses

Element spacing =  $.5\lambda$

Samples = 64 (8N)

Scan Angle =  $0^\circ$

Interpulse motion =  $.2 \lambda/\text{pulse}$

Runs = 4

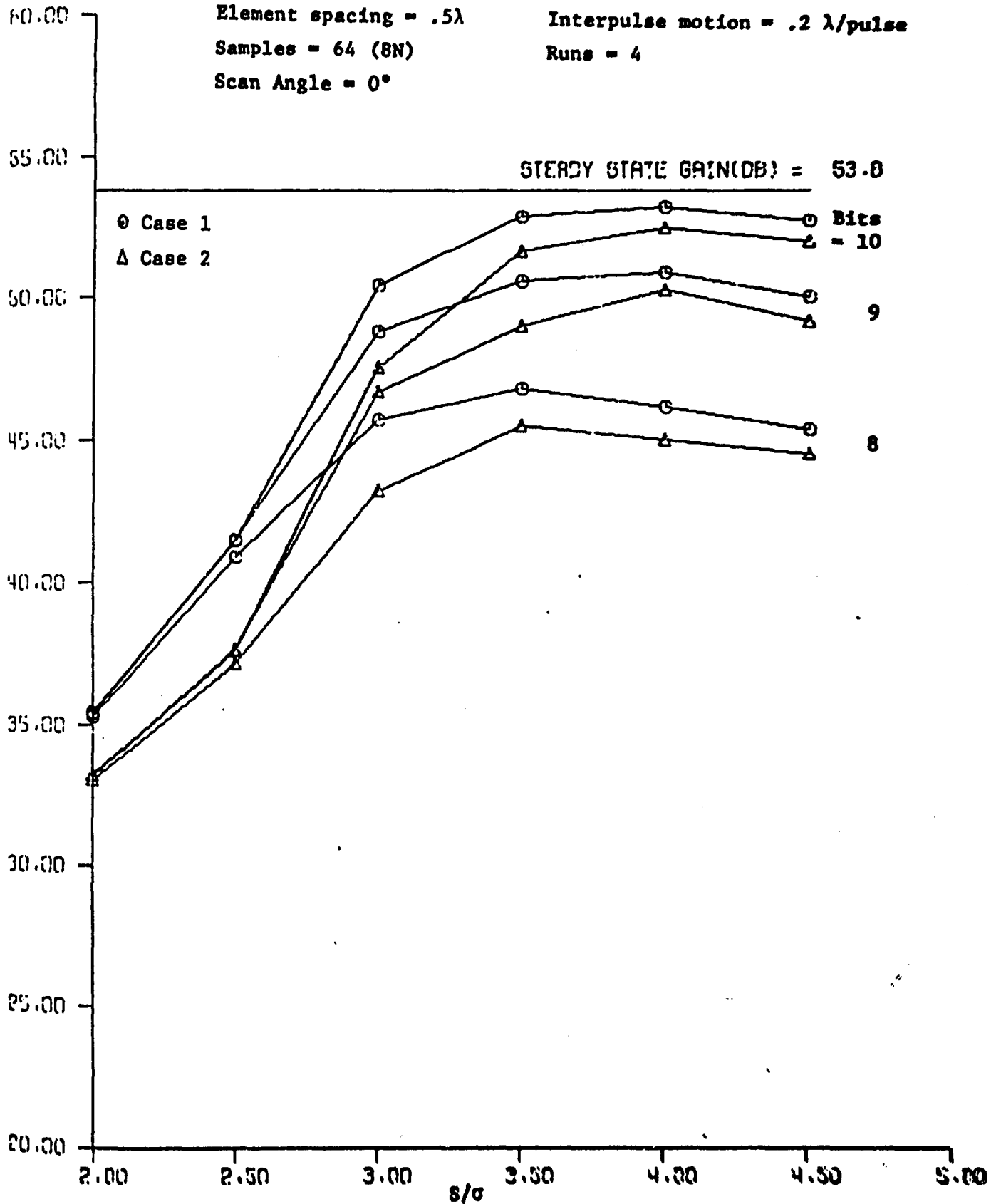


Figure 2.5 MTI Gain vs. Envelope Limit Level and Number of Bits

4 elements 2 pulses

Element spacing =  $.5\lambda$

Interpulse motion =  $.23\lambda/\text{pulse}$

Samples = 32

Runs = 4

Scan Angle =  $90^\circ$

STEADY STATE GAIN (DB) = 68.0

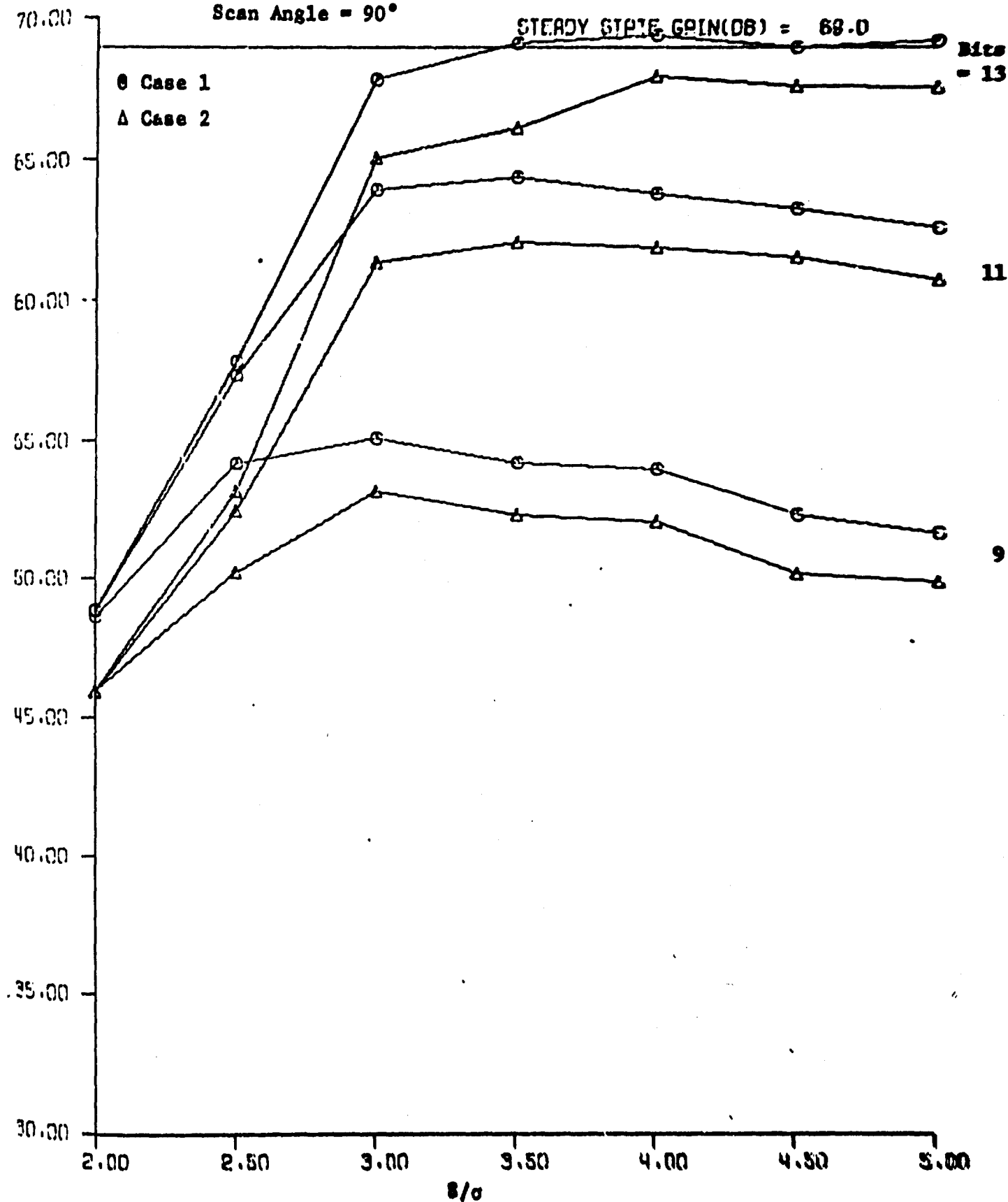


Figure 2.6 MTI Gain vs. IQ Limit Level and Number of Bits

4 elements 2 pulses

Element spacing =  $.5\lambda$

Interpulse motion =  $.23\lambda/\text{pulse}$

Samples = 32

Runs = 4

Scan Angle =  $90^\circ$

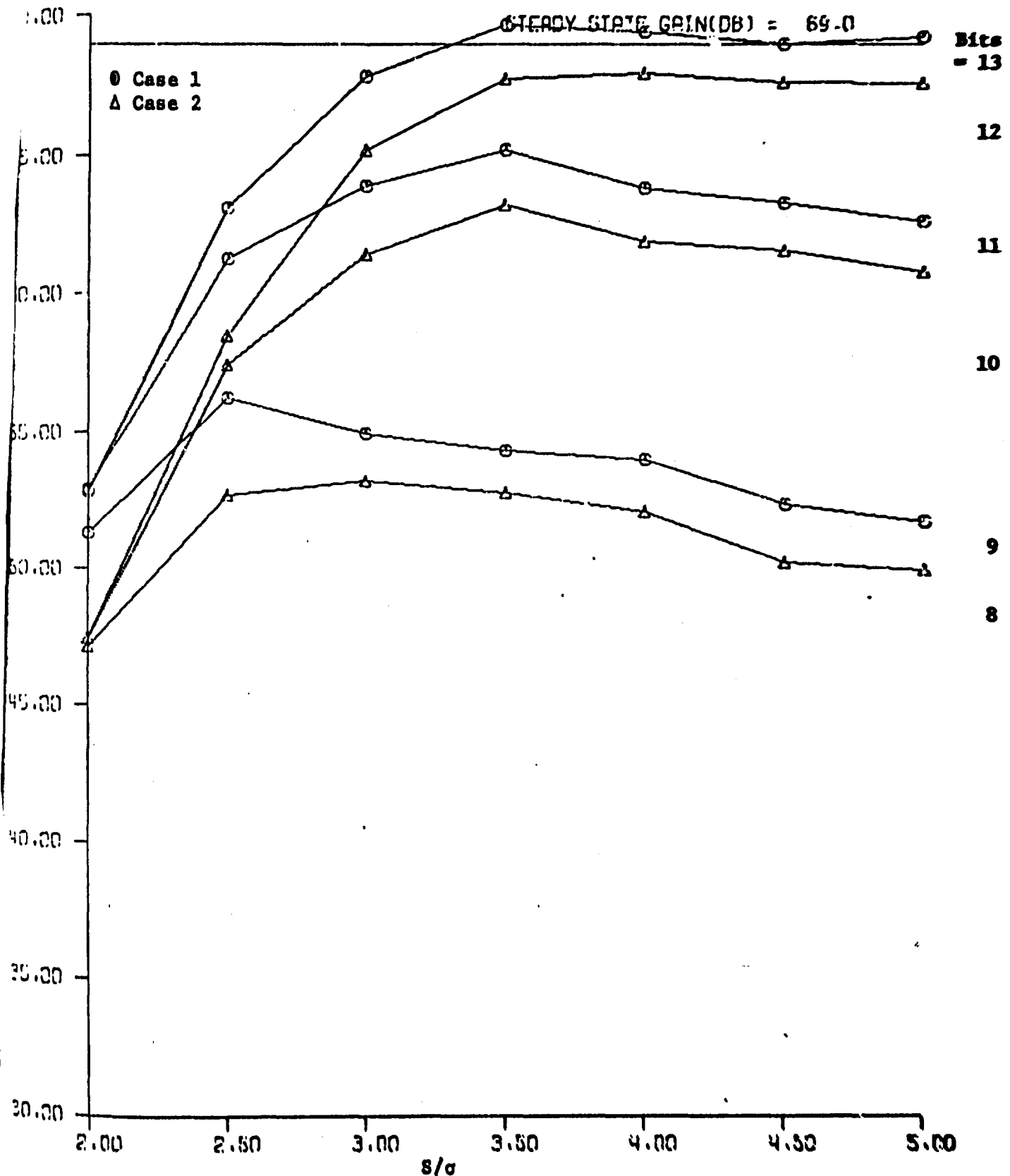


Figure 2.7 MTI Gain vs. Envelope Limit Level and Number of Bits

is possible since the weights are determined for a particular set of samples and used on the same sample set.

In Figure 2.8 the same example is used as in Figures 2.6 and 2.7 but the range of  $S/\sigma$  is extended and different numbers of bits are used. This Figure shows clearly, that while there is an optimum ratio of limit level  $S$  to average voltage  $\sigma$ , the optimum is quite broad, and performance declines slowly with increasing values of  $S/\sigma$ . This shows that it is clearly better to operate in a region of low limiting, and to bias the operating point toward the high side of  $S/\sigma$  when  $\sigma$  is changing rapidly or is not accurately known.

Figure 2.9 shows similar results for a lower performance level.

4 elements 2 pulses

Element spacing =  $.5\lambda$

Interpulse motion =  $.23\lambda/\text{pulse}$

Samples = 32

Runs = 4

Scan Angle =  $90^\circ$

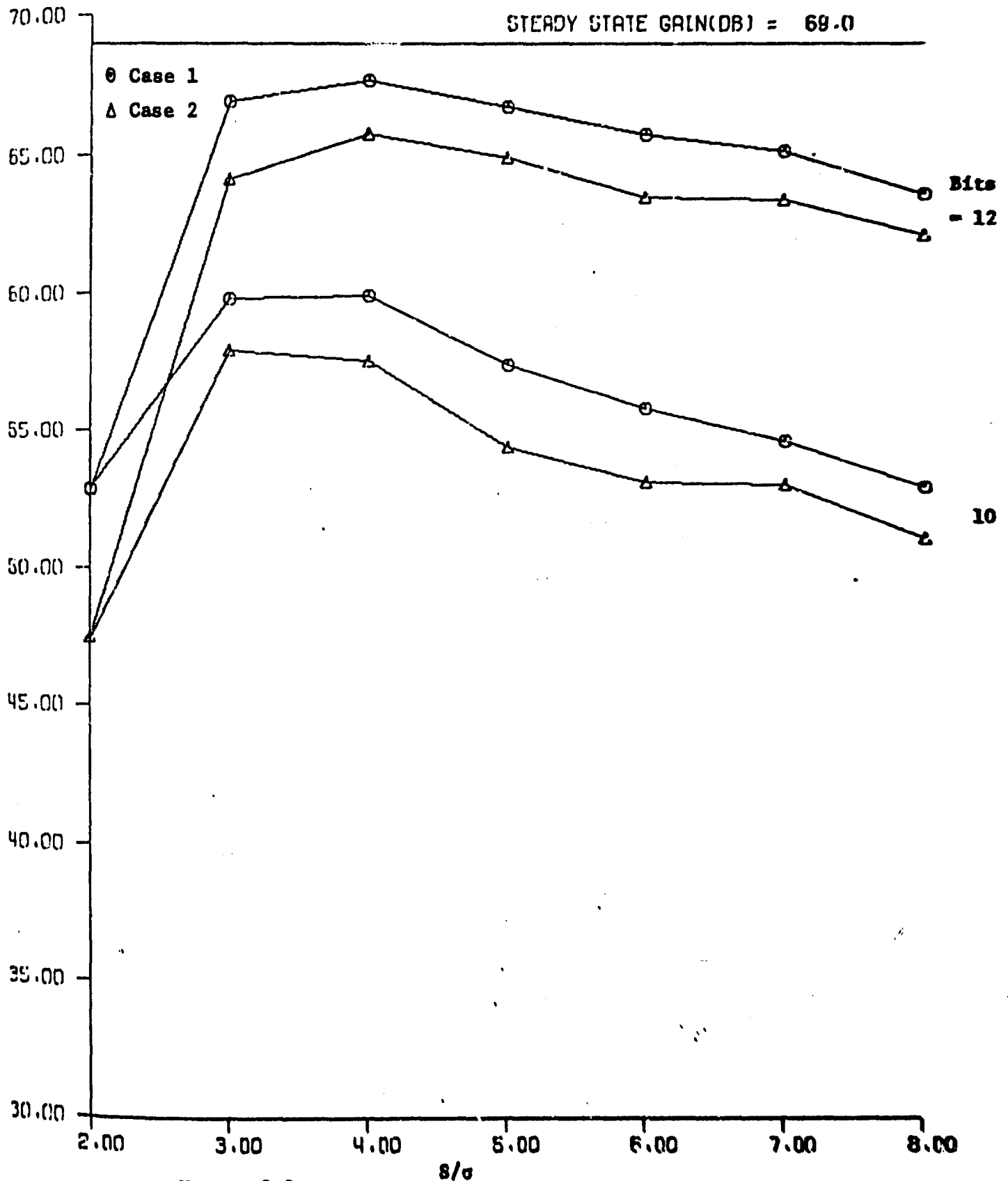


Figure 2.8 NTI Gain vs. IQ Limit Level and Number of Bits

4 elements 2 pulses

Element spacing =  $.5\lambda$

Samples = 32 (4N)

Scan Angle =  $90^\circ$

Interpulse motion =  $.625\lambda/\text{pulse}$

Runs = 4

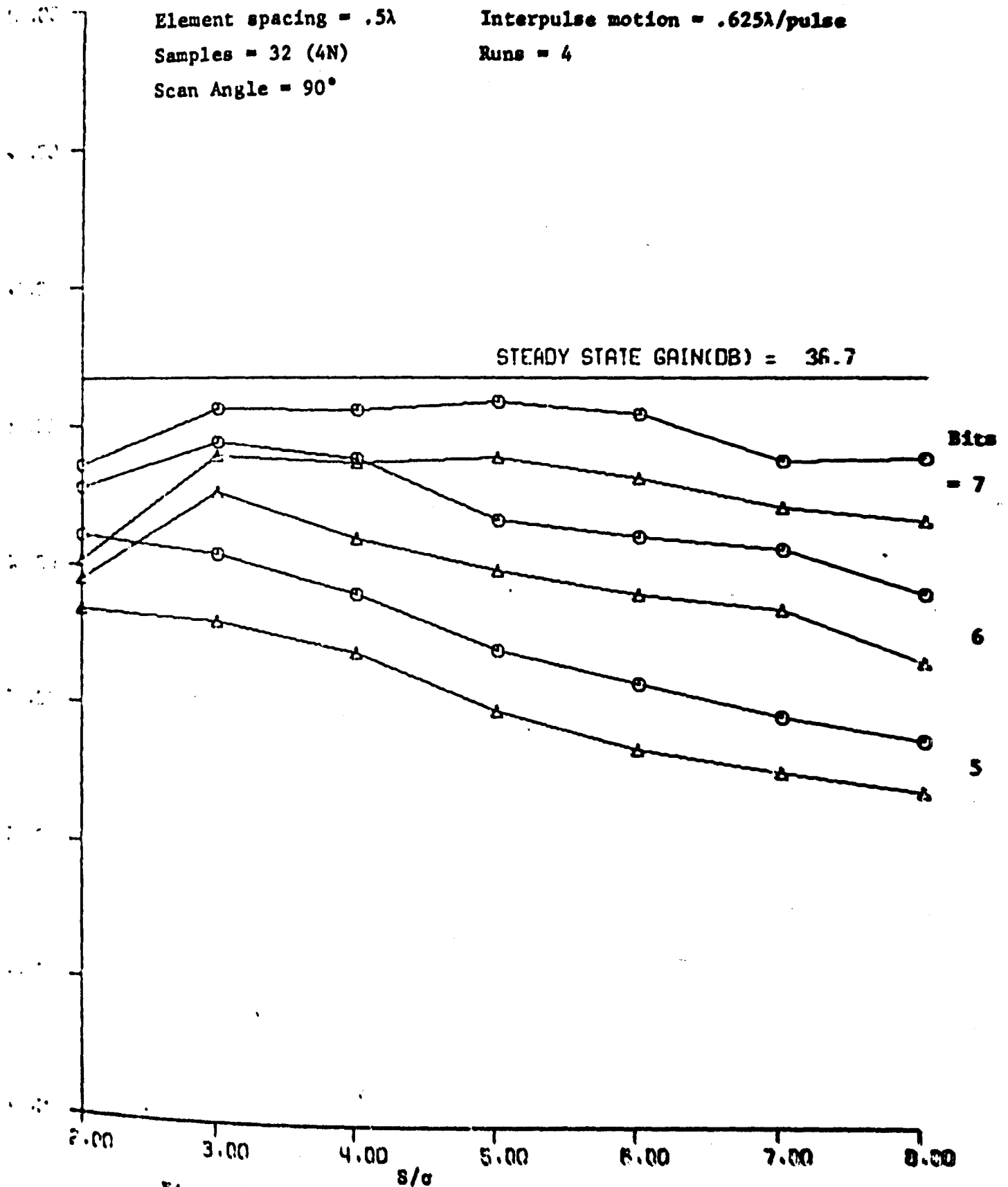


Figure 2.9 MTI Gain vs. IQ Limit and Number of Bits

### 3.0 SOME CONVERGENCE EXPERIMENTS

In the first progress report<sup>[3]</sup> the convergence rates of three algorithms were compared using a computer simulation. The sample matrix inversion (SMI) and inverse matrix update (IMU) techniques were shown to be comparable and very fast when measured by the number of independent data samples required to converge. The Applebaum loop, while much simpler to implement, converges much more slowly requiring hundreds of samples, in the example shown, compared to two to four times the number of degrees of freedom,  $N$ , required by SMI and IMU.

The SMI technique is known to require the least number of samples under all conditions, and requires only  $N(N+1)/2$  complex multiplications to form  $\hat{M}$ <sup>[5]</sup>. These properties are invariant over all problems, thereby making the technique extremely powerful.

To invert the matrix  $\hat{M}$  for SMI requires about  $N^3/3$  multiplications or divisions. There are several ways of doing this, i.e. solving the set of simultaneous equations required to obtain the weights, or inverting the matrix by various methods. Computational problems may be involved in the SMI or IMU technique when high speed and limited numbers of bits is a requirement.

The IMU algorithm is simple to program, requiring only about  $1.75 N^2 + 2.75 N$  complex multiplications, per data sample. This can be seen from the recursive equation:

$$M_{j+1}^{-1} = \frac{1}{(1-\alpha)} M_j^{-1} - \frac{\alpha}{1-\alpha} \frac{(M_j^{-1} V^*) (V_T M_j^{-1})}{(1-\alpha) + \alpha (V_T M_j^{-1} V^*)} \quad (3-1)$$

where the sample matrix is given by

$$M_{j+1} = (1-\alpha)M_j + \alpha V_j^* V_{jT} \quad (3-2)$$

Basically  $M_j^{-1} V^*$  is formed using  $N^2$  multiplications,  $V_T M_j^{-1}$  is formed by taking its conjugate, and to obtain  $V_T M_j^{-1} V^*$  requires a further  $N$  multiplications. Since  $M_j^{-1}$  is Hermitian, multiplying  $M_j^{-1} V^*$  by  $V_T M_j^{-1}$  requires  $N(N+1)/2$  multiplications. Finally multiplying by the constants provides for the remaining multiplications.

The simplicity of implementing IMU makes it interesting to see how many samples are required for convergence both as a function of  $\alpha$  and of the starting values of  $M_j^{-1}$ . For fixed values of  $\alpha$  an exponential weighting is applied to the incoming data samples as they are used to update the matrix. When  $\alpha = \frac{1}{j+1}$ , equal weighting is applied to the data samples used to update  $M^{-1}$ .

The starting values of  $M^{-1}$  are less easily parameterized since they could be anything from an arbitrary choice to a choice which is close to the correct value. To explore IMU as a function of the initial matrix  $M_0^{-1}$  one wishes to construct a problem related to a practical radar situation in which external interference (clutter, jamming etc.) is changing. Also one would like the weights to change in such a manner that a required performance is maintained. For example, one might require the weights to

adjust as the antenna rotates between pulse groups. This was treated in the first progress report<sup>[3]</sup>. For another example, one might require the weights to change with the changes in clutter with range as treated in a previous TSC study<sup>[6]</sup>. The latter might be caused by terrain changes such as a land to sea interface.

In these experiments antenna step scanning was assumed in such a manner that the weights are optimized at one angle, then the antenna is rotated to a new angle and held fixed while new samples are taken. In Figure 3.1 the IMU process is started with the diagonal having the same values as the diagonal of the inverted matrix  $M_0^{-1}$  for the previous angle. The inverse matrix is then updated with the new data, using  $\alpha = \frac{1}{j+1}$ , i.e., giving equal weight to each new sample.

A large rotation angle  $5^\circ$  was chosen to accentuate the mismatch. The results for the IMU and SMI techniques are seen to be quite similar. The loop convergence performance is also shown for the case where steady state performance was reached at the previous angle. The gain/TAU ratio is adjusted so that control loop noise in the steady state increases the total output noise by 25%<sup>[7]</sup>.

It seemed reasonable that if the entire inverse matrix for a previous starting angle were used, that the results would be equally good if not better. Figure 3.2 shows that this is not the case, at least for this example. The IMU performance was considerably degraded when the ideal  $M_0^{-1}$  for the previous angle was used as the initial matrix.

Figures 3.3 and 3.4 show that using the previous inverse matrix diagonal even when it is multiplied by .1 or 10 gives extremely good agreement between the SMI and IMU techniques.

Figure 3.1 ADAPTIVE ARRAY/DOPPLER PROC.

GAIN= 1000

TAU= 2449423

4 ELEMENTS

2 PULSES

ELEMENT SPAC= .5

INTERPULSE MOTION= .2000

SCAN ANGLE(DEG)= 90.0

ROTATION(DEG)= 5.000

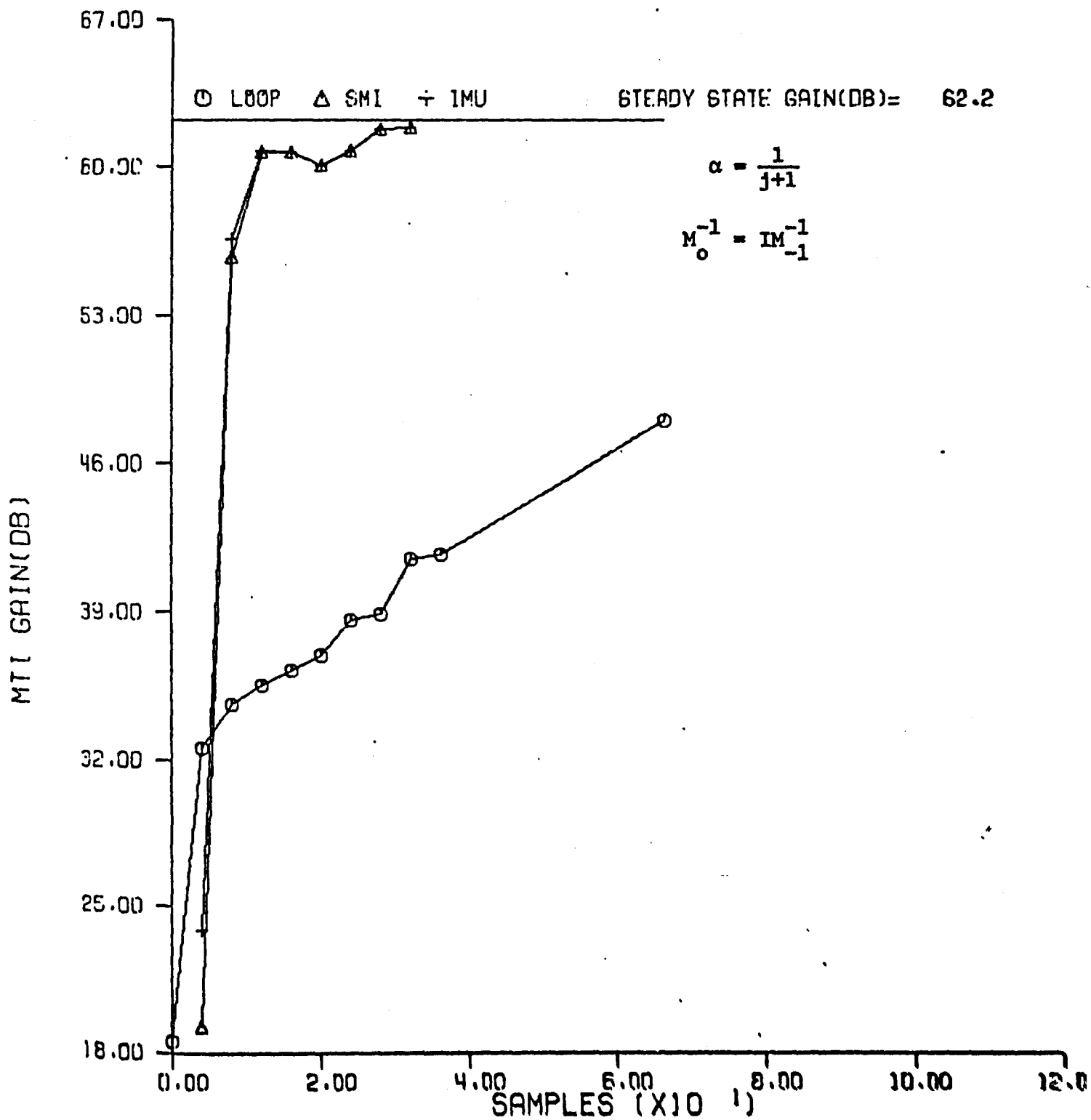


Figure 3.2 ADAPTIVE ARRAY/DOPPLER PROC.

GAIN= 1000

TAU= 2449423

4 ELEMENTS

2 PULSES

ELEMENT SPAC= .5

INTERPULSE MOTION= .2000

SCAN ANGLE(DEG)= 90.0

ROTATION(DEG)= 5.000

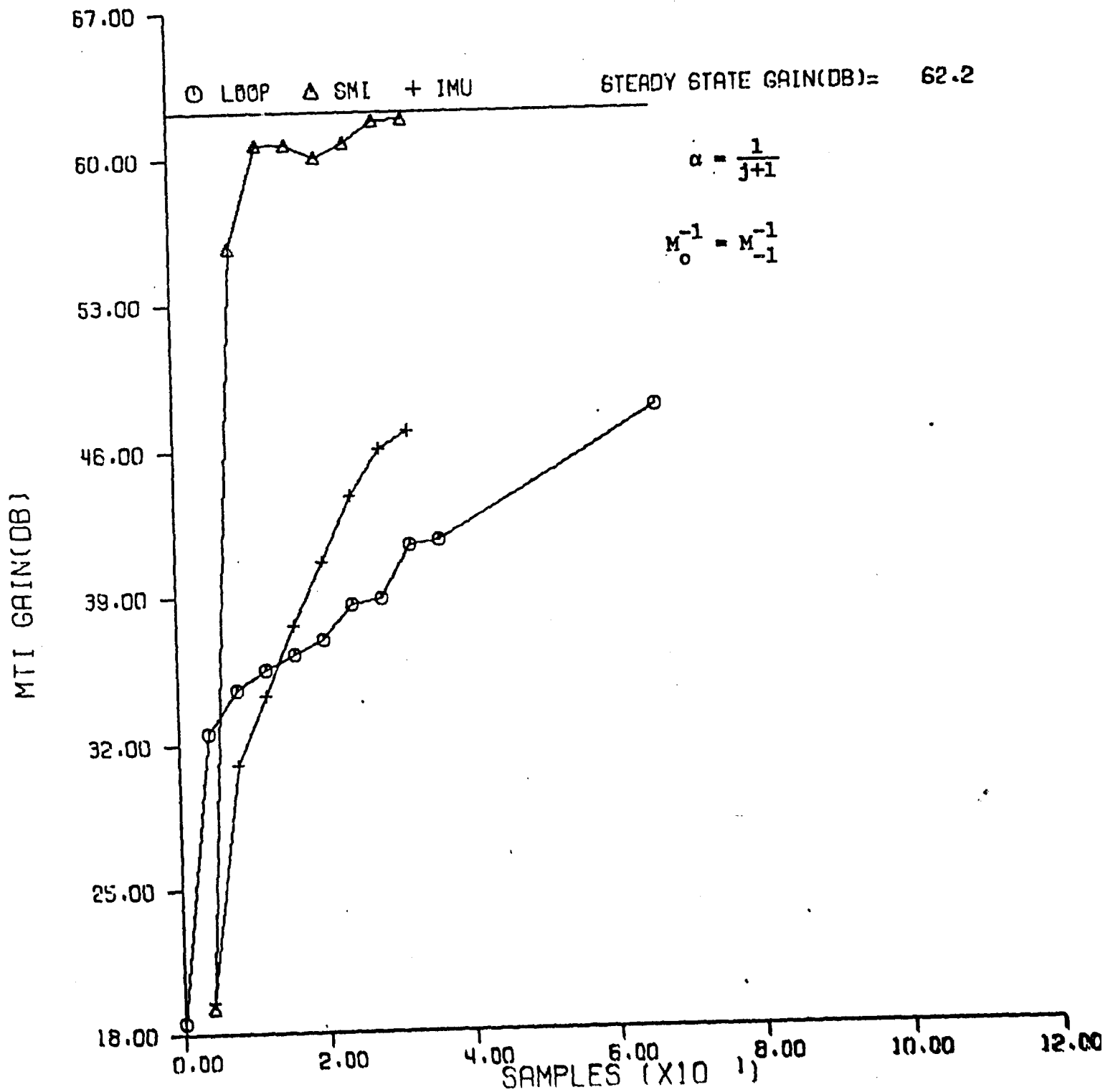


Figure 3.3 ADAPTIVE ARRAY/DOPPLER PROC.

GAIN= 1000

TAU= 2449123

4 ELEMENTS

2 PULSES

ELEMENT SPAC= .5

INTERPULSE MOTION= .2000

SCAN ANGLE( DEG)= 90.0

ROTATION( DEG)= 5.000

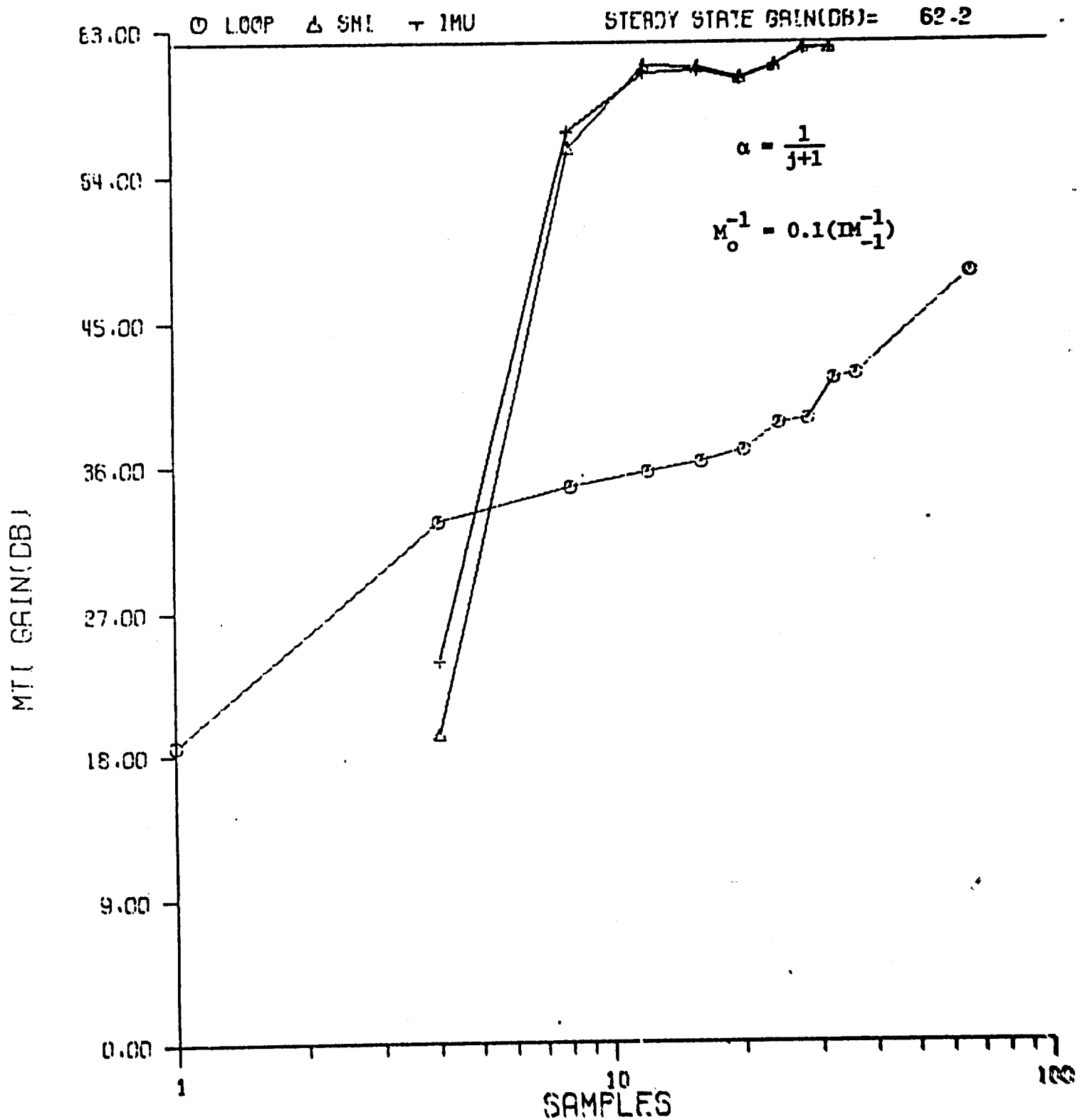
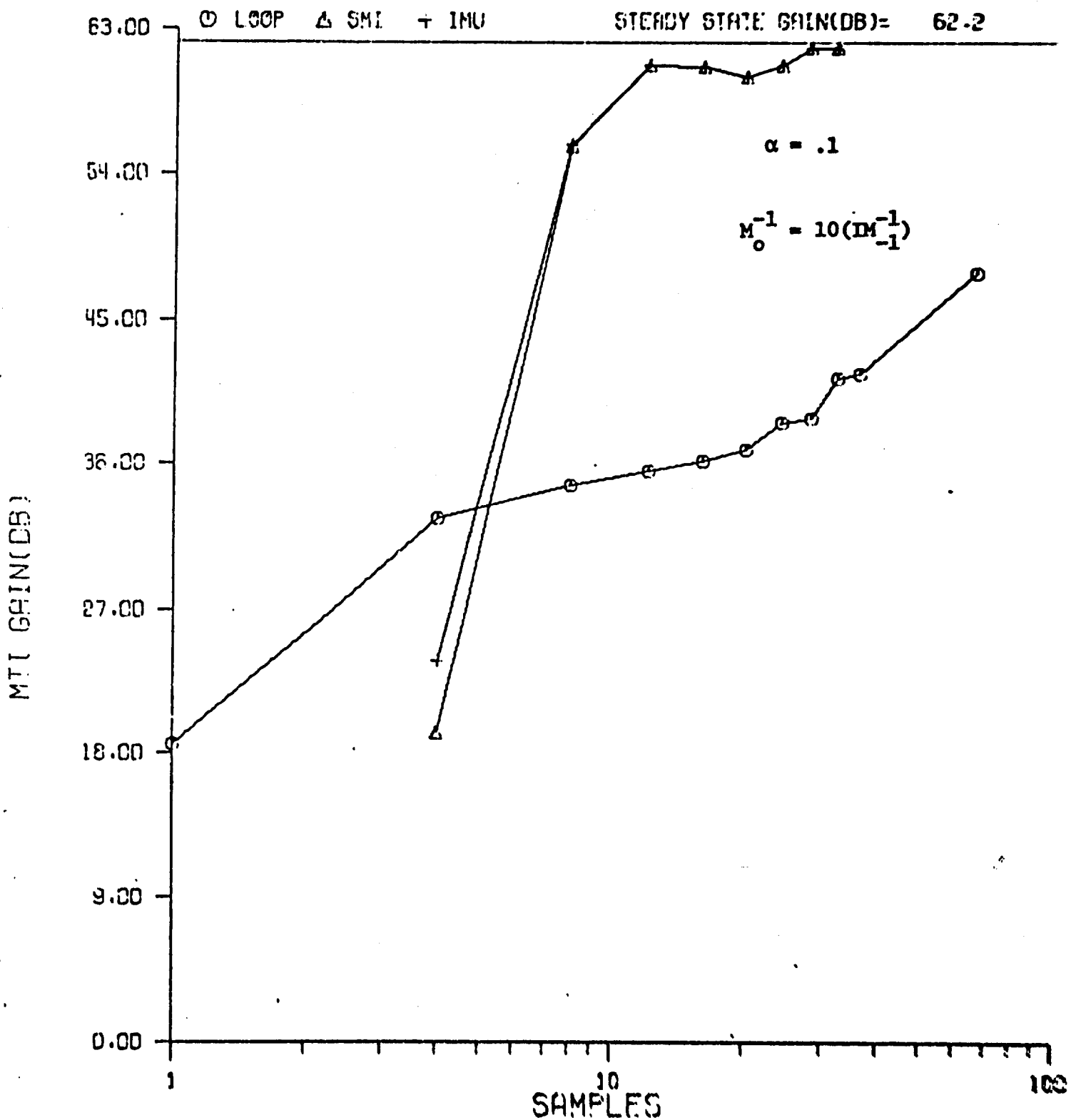


Figure 3.4 ADAPTIVE ARRAY/DOPPLER PROC.

GAIN= 1000                      TAU= 24-19423  
4 ELEMENTS                      2 PULSES  
ELEMENT SPAC= .5                INTERPULSE MOTION= .2000  
SCAN ANGLE(DEG)= 90.0            ROTATION(DEG)= 5.000



In Figure 3.5 - 3.7 different values of  $\alpha$  are shown using the diagonal of the previous updated matrix.

These figures indicate that constant values of  $\alpha$  are much less desirable than the varying value which gives equal weighting to the samples. This is what would be expected in the step scan example, assumed in this case. If a steady scan rate were used and data were taken from many range traces, then an optimum constant value for  $\alpha$  could be found.

The simulation program ADAPTM6 listed in the first progress report<sup>[3]</sup> was used in these experiments.

Figure 3.5 ADAPTIVE ARRAY/DOPPLER PROC.

GRIN= 1000

TAU= 2449423

4 ELEMENTS

2 PULSES

ELEMENT SPAC= .5

INTERPULSE MOTION= .2000

SCAN ANGLE(DEG)= 90.0

ROTATION(DEG)= 5.000

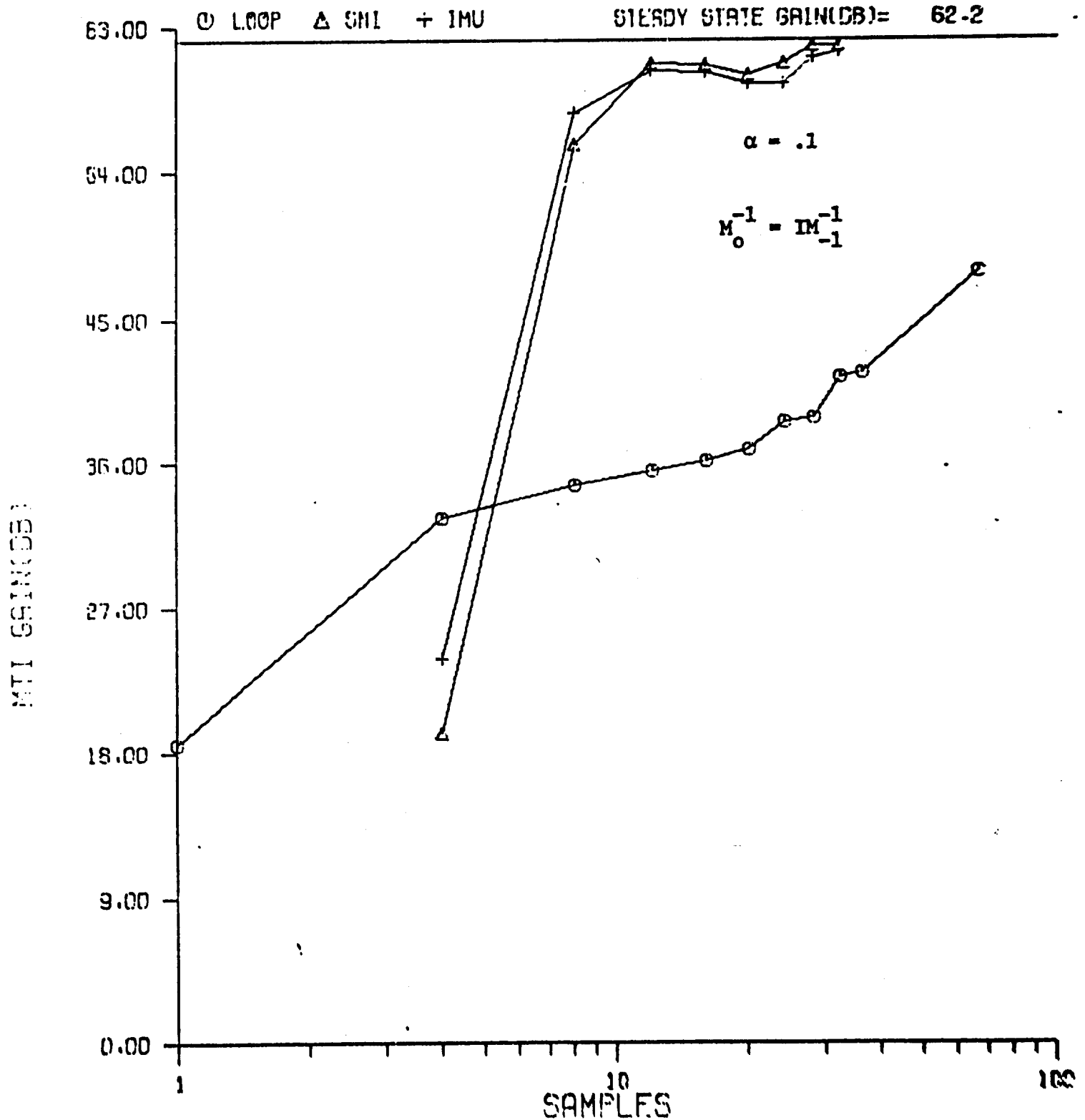


Figure 3.6 ADAPTIVE ARRAY/DOPPLER PROC.

GAIN= 1000                      TAU= 2449423  
 4    ELEMENTS                      2    PULSES  
 ELEMENT SPAC= .5                  INTERPULSE MOTION= .2000  
 SCAN ANGLE( DEG)= 90.0                  ROTATION( DEG)= 5.000

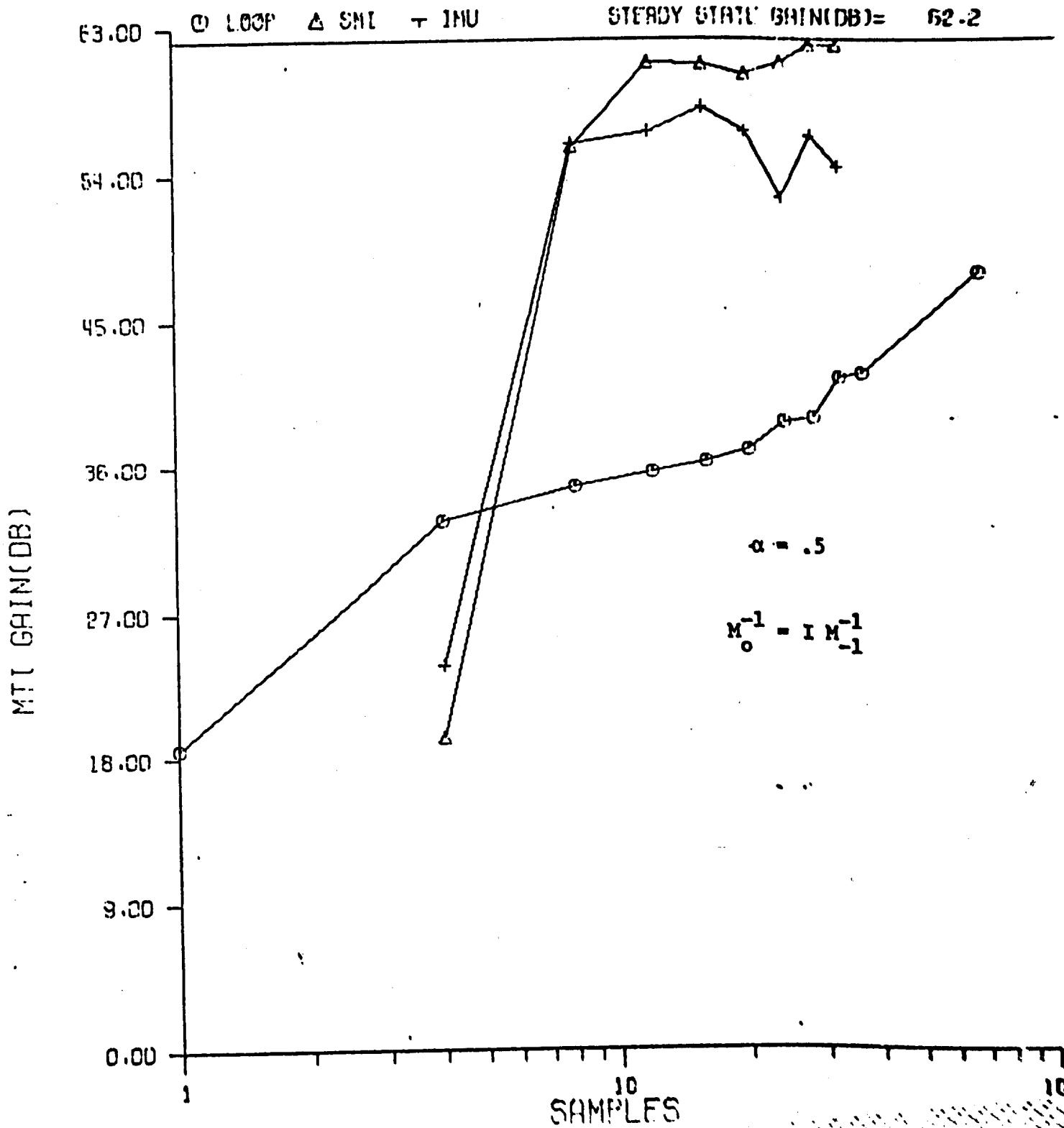


Figure 3.7 ADAPTIVE ARRAY/DOPLER PROC.

GAIN= 1000

TAU= 2449423

4 ELEMENTS

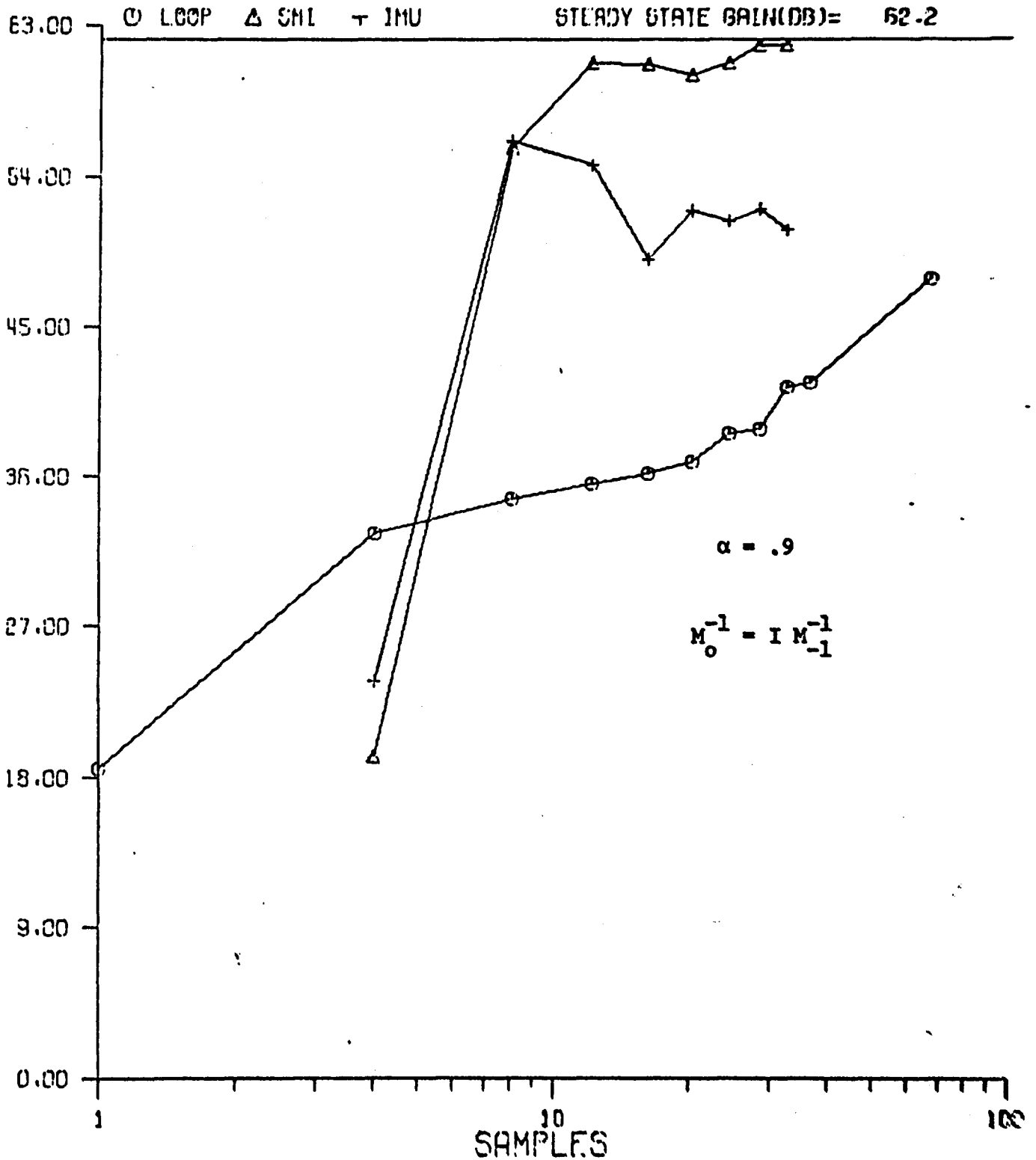
2 PULSES

ELEMENT SPAC= .5

INTERPULSE MOTION= .2000

SCAN ANGLE(DES)= 90.0

ROTATION(DES)= 5.000



REFERENCES

1. "Adaptive Array Techniques for Coherent Airborne Radars," Technology Service Corp., TSC-PD-030-1, 26 February 1970, Final Report on Contract N00019-69-C-0662.
2. "ADAPTAR Space-Time Processing in Airborne Radars," Technology Service Corp., TSC-PD-061-2, 24 February 1971, Final Report on Contract N00019-70-C-0387.
3. "Convergence Rate in Adaptive Radar", TSC-PD-137-1, 27 February 1975.
4. L. E. Brennan and I. S. Reed, "Theory of Adaptive Radar", IEEE Trans. of Aerospace & Electronic Systems, VOL. AES-9, No. 2, March 1973.
5. I. S. Reed, J. D. Mallett, L. E. Brennan, "Rapid Convergence Rate in Adaptive Arrays," IEEE Trans. of Aerospace & Electronic Systems, Vol. AES-10, No. 6, Nov. 1974.
6. I. S. Reed, J. D. Mallett, L. E. Brennan, "Adaptive Radar Techniques", TSC-PD-096-2, April 27, 1973.
7. L. E. Brennan and I. S. Reed, "Quantization Noise in Digital Moving Target Indication Systems," IEEE Trans. on Aerospace & Electronic Systems, Vol. AE5-2, No. 6, Nov. 1966.
8. L. E. Brennan, I. S. Reed, and E. Pugh, "Control Loop Noise in Adaptive Array Antennas," IEEE Trans. AES, March 1971, pp. 254-262.
9. L. E. Brennan, I. S. Reed, "Effect of Envelope Limiting in Adaptive Array Control Loops," IEEE, Vol. AES-7, July 1971.

APPENDIX ILOSSES IN ADAPTIVE RADAR PERFORMANCE DUE TO QUANTIZATIONPRELIMINARIES

Analyses of adaptive radar performance usually neglect the detailed effects of quantization noise. If estimates of degradation in performance are made, they often depend on costly computer simulations. This situation is improved here for most cases of practical interest by developing formulas for computing the signal-to-noise loss in adaptive radar performance due to quantization.

Assume the adaptive array-radar has a receiving array of  $M$  identical elements. Let  $z_k(t)$  be the complex-valued process received by the  $k$ -th element for  $k=1,2,\dots,M$ . In a pulse-sampling radar, pulses are transmitted periodically with pulse repetition period  $T$ . For this case the reflected signals from an object at fixed range  $R = \frac{c\tau}{2}$  are proportional to the coefficient of reflectivity of that object. Here, of course,  $\tau$  is the round-trip time required for a pulse to travel from the radar antenna to the object and return, and  $c$  is the velocity of light. Such a radar samples the reflectivity of the object sequentially at times  $t_1, t_2, \dots, t_L$  where  $t_n = nT$ . The sampled data set associated with these sampling times is the sampled data set  $\{z_k(t_n)\}$  of signals received from an object at range  $R$ . It is convenient for mathematical purposes to represent this sampled-data set as the column vector (matrix),

$$\begin{pmatrix} z_1(t_1) \\ \vdots \\ z_M(t_1) \\ \vdots \\ z_1(t_L) \\ \vdots \\ z_M(t_L) \end{pmatrix} \equiv \begin{pmatrix} x_1 \\ \vdots \\ x_M \\ \vdots \\ x_{(L-1)M+1} \\ \vdots \\ x_{ML} \end{pmatrix} \equiv X$$

where  $N = M \times L$  is the number of dimensions of the vector.

Radar detection involves a choice between two hypotheses, the noise-only hypothesis  $H_0$  and the signal-plus-noise hypothesis  $H_1$ . Assuming additive Gaussian noise of zero mean, the expected value of  $X$ , given hypothesis  $H_0$  (noise only), is

$$EX = 0.$$

Similarly the expected value of  $X$ , given  $H_1$  (signal plus noise) is

$$EX = S$$

where  $S$  is the column vector (matrix)

$$S = \begin{pmatrix} s_1 \\ s_2 \\ \vdots \\ s_N \end{pmatrix}$$

of signal echoes that might be expected from an object at range  $R$  at the  $M$  elements of the array from the  $L$  pulses. For hypothesis  $H_1$ , the noise vector is given by  $N = X - S$ . Assume that all components of  $M$  are Gaussian and jointly distributed.

In order to detect signal vector  $S$  in the received sampled-data vector  $X$  one must design a filter (a linear functional) for vector  $X$  which is tuned to signal  $S$ . Such a sampled-data filter is the scalar

$$y = \sum_{k=1}^N \bar{w}_k x_k = W^* X \quad (1)$$

where  $W$  is the weight vector

$$W = \begin{pmatrix} w_1 \\ w_2 \\ \vdots \\ w_N \end{pmatrix}$$

of complex numbers,  $\bar{w}_k$  denotes complex conjugation and  $W^*$  denotes the conjugate transpose of the column matrix  $W$ .

## 2.2 MOMENTS OF QUANTIZED VIDEO

To study the effects of quantization on adaptive radar performance one needs to find the moments of the sample data filter  $y$ , given in (1). To treat this problem let  $[x_n] = [u_n] + i[v_n]$  be the quantized or digitalized value of the complex number  $x_n = u_n + iv_n$  where  $[v_n]$  denotes the digital value of the imaginary part of  $x_n$ . In the conversion from analog to digital let

$$[x_n] = x_n + \varepsilon(x_n) \quad (2)$$

where

$$\varepsilon(x_n) = e(u_n) + i e(v_n) \quad (3)$$

is the complex error. Here  $e(u_n)$  is the real part of  $\varepsilon(x_n)$  and  $e(v_n)$  is the imaginary part of error  $\varepsilon(x_n)$  in the A-D conversion process. The error functions  $e(u)$  and  $e(v)$  are sawtooth functions of the real and imaginary parts of  $x = u + iv$ , respectively. Explicitly,  $e(u)$  and  $e(v)$  have the same Fourier series representation, given by

$$e(u) = \frac{\Delta}{\pi} \sum_{k=1}^{\infty} \frac{(-1)^k}{k} \sin\left(\frac{2\pi ku}{\Delta}\right) \text{ and} \quad (4)$$

$$e(v) = \frac{\Delta}{\pi} \sum_{k=1}^{\infty} \frac{(-1)^k}{k} \sin\left(\frac{2\pi kv}{\Delta}\right),$$

respectively, where  $\Delta$  is the quantizer step size in voltage [see Reference 1].

For signal-plus-noise the first moment of  $[x_n]$ , the quantized version of the  $n$ -th component of the sampled-data vector  $X$ , is by (2) and (3)

$$\begin{aligned} E[x_n] &= E(x_n + \varepsilon(x_n)) \\ &= E x_n + E(\varepsilon(x_n)) \\ &= s_n + E e(u_n) + i E e(v_n) \end{aligned}$$

Replacing  $e(\sigma)$  and  $e(\tau_n)$  by their Fourier series, eq. (4), and inverting the order of the summation and expected value operator  $E$ , yields

$$E[x_n] = s_n + \Delta \sum_{k=1}^{\infty} \frac{(-1)^k}{k} E \left\{ \sin \frac{2\pi k}{\Delta} u_n + i \sin \frac{2\pi k}{\Delta} v_n \right\}$$

Since  $\sigma_n$  and  $\tau_n$  are independent identically distributed Gaussian variates with means  $R(s_n)$  and  $I(s_n)$ , respectively, where  $R(s_n)$  and  $I(s_n)$  are the real and imaginary components of signal component  $s_n$ ,

$$\begin{aligned} E \sin \left( \frac{2\pi k}{\Delta} u_n \right) &= \frac{1}{\sqrt{2\pi\sigma}} \int_{-\infty}^{\infty} e^{-\frac{(u_n - R s_n)^2}{2\sigma^2}} e^{i \frac{2\pi k}{\Delta} u_n} du_n \\ &= e^{-2\pi^2 k^2 (\sigma/\Delta)^2} \sin \left( \frac{2\pi k R(s_n)}{\Delta} \right) \end{aligned}$$

and

$$E \sin \left( \frac{2\pi k}{\Delta} v_n \right) = e^{-2\pi^2 k^2 (\sigma/\Delta)^2} \sin \left( \frac{2\pi k I(s_n)}{\Delta} \right)$$

Thus

$$E[x_n] = s_n + \frac{\Delta}{\pi} \sum_{k=1}^{\infty} \frac{(-1)^k}{k} e^{-2\pi^2 k^2 (\sigma/\Delta)^2}$$

$$\times \left( \sin \frac{2\pi k R(s_n)}{\Delta} + i \sin \frac{2\pi k I(s_n)}{\Delta} \right)$$

where  $R(s_n)$  and  $I(s_n)$  are the real and imaginary components of the  $n$ -th component  $s_n$  of the signal vector  $S$  and  $\sigma$  is the standard deviation of the noise.

For most cases of practical interest in adaptive radar  $\Delta \ll \sigma$ .

For this case

$$E[x_n] = s_n + O\left(e^{-2\pi^2\left(\frac{\sigma}{\Delta}\right)^2}\right)$$

where  $O(y)$  denotes the order of  $y$  as  $y$  tends to zero. Evidently

$E[x_n]$  is closely approximated on the average by the  $s_n$ , i.e.  $E[x_n] \approx s_n$ .

The complex covariance matrix of  $[X]$ , the quantized version of the data vector  $X$  for noise alone is by (3)

$$\begin{aligned} M_Q &= E[X][X]^* \\ &= E(X + \epsilon(X))(X + \epsilon(X))^* \\ &= EXX^* + E\epsilon(X)\{\epsilon(X)\}^* + E(\{\epsilon(X)\}X^* + X\{\epsilon(X)\}^*) \end{aligned}$$

(5)

where  $*$  denotes conjugate transpose and  $\epsilon(X)$  is the column vector of complex quantization errors  $\epsilon(x_n)$ , as given by (3), namely,

$$\epsilon(X) = \begin{pmatrix} \epsilon(x_1) \\ \epsilon(x_2) \\ \vdots \\ \epsilon(x_N) \end{pmatrix}$$

The first term of (5) is the covariance matrix  $M$  of the sample-data vector  $X$ , i.e.,

$$M = E\{X X^*}$$

To treat the second term of (5) and make use of previous results, we must transform the data sample vector,

$$X = \begin{pmatrix} x_1 \\ x_2 \\ \vdots \\ \vdots \\ x_N \end{pmatrix} = \begin{pmatrix} u_1 + iv_1 \\ u_2 + iv_2 \\ \vdots \\ \vdots \\ u_N + iv_N \end{pmatrix} = V + iV \quad (6)$$

of  $n$  complex components into the data sample vector

$$U = \begin{pmatrix} y_1 \\ y_2 \\ \vdots \\ \vdots \\ y_{2N} \end{pmatrix} = \begin{pmatrix} u_1 \\ u_2 \\ \vdots \\ \vdots \\ u_N \\ v_1 \\ v_2 \\ \vdots \\ \vdots \\ v_N \end{pmatrix} = \begin{pmatrix} U \\ V \end{pmatrix} \quad (7)$$

of  $2N$  real components where  $u_k$  is the real part of sample  $x_n$ ,  $v_k$  is the imaginary part of sample  $x_k$ , and

$$U = \begin{pmatrix} u_1 \\ u_2 \\ \cdot \\ \cdot \\ u_N \end{pmatrix} \quad \text{and} \quad V = \begin{pmatrix} v_1 \\ v_2 \\ \cdot \\ \cdot \\ v_N \end{pmatrix}$$

are the real and imaginary parts of  $X$ , respectively.

Let also the complex covariance matrix  $M$  and its inverse  $M^{-1}$  be decomposed into real and imaginary parts as

$$M = A + iB \quad \text{and} \quad M^{-1} = C + iD \quad (8)$$

Then the  $2N \times 2N$  symmetric matrix

$$V = \begin{pmatrix} A, & -B \\ B, & A \end{pmatrix} = EY Y^T \quad (9)$$

has the inverse

$$V^{-1} = \begin{pmatrix} C, & -D \\ D, & C \end{pmatrix} \quad (10)$$

where  $Y^T$  denotes the transpose of vector  $Y$ .

Next, the quadratic form  $X^* M^{-1} X$  can be shown to be identical to the quadratic form  $Y^T X^{-1} Y$  where  $X^{-1}$  is given by (9). To show this

$$\begin{aligned} X^* M^{-1} X &= (U + iV) (C + iD) (U + iV) \\ &= (U - iV)^T (C + iD) (U + iV) \\ &= (U - iV^T) (C + iD) (U + iV) \\ &= U^T C U + V^T D U - U^T D V + V^T C V \end{aligned}$$

where the imaginary part vanishes since  $M^{-1}$  is Hermitian and where  $U^T$  denotes the transpose of the real vector  $U$ . Similarly

$$\begin{aligned} Y^T X^{-1} Y &= \begin{pmatrix} U \\ V \end{pmatrix}^T \begin{pmatrix} C & -D \\ D & C \end{pmatrix} \begin{pmatrix} U \\ V \end{pmatrix} \\ &= (U^T C + V^T D, -U^T D + V^T C) \begin{pmatrix} U \\ V \end{pmatrix} \\ &= U^T C U + V^T D U - U^T D V + V^T C V \end{aligned}$$

Since this agrees with the above, the identity

$$X^* M^{-1} X = Y^T K^{-1} Y \quad (11)$$

is true. The joint probability density of the components of the vector  $X$  is

$$P(X) = (\pi)^{-n} |M|^{-1} \exp(-X^* M^{-1} X) \quad (12)$$

where  $|M|$  is the determinant of the covariance matrix  $M$ . Using (11), this density is easily shown to be equivalent to the density

$$P(Y) = (\pi)^{-M} |K|^{-1/2} \exp(-Y^* K^{-1} Y) \quad (13)$$

where  $Y$  is the  $2n$  component vector, given by (7) and  $K^{-1}$  is defined by (9).

The above remarks will now be used to evaluate the second term of (5). The  $(m,n)^{\text{th}}$  element of this is

$$\begin{aligned} E\left(\varepsilon(x_m) \overline{\varepsilon(x_n)}\right) &= E\left(e(u_m) + ie(v_m)\right) \left(e(u_n) - ie(v_n)\right) \\ &= E e(u_m) e(u_n) + E e(v_m) e(v_n) \\ &\quad + i\left(E e(u_m) e(v_n) - E e(u_n) e(v_m)\right) \\ &= 2\left(E e(u_m) e(u_n) + i E e(u_m) e(v_n)\right) \end{aligned} \quad (14)$$

where the last line follows from (9). The first term of (14) is

$$\begin{aligned} E e(u_m) e(u_n) &= \int_{-\infty}^{\infty} \int_{-\infty}^{\infty} P(u_m, u_n) e(u_m) e(u_n) du_m du_n \\ &= \left(\frac{\Delta}{\pi}\right)^2 \sum_{k=1}^{\infty} \sum_{\ell=1}^{\infty} \frac{(-1)^{k+\ell}}{k\ell} I_{k\ell} \end{aligned}$$

where

$$I_{k\ell} = \int_{-\infty}^{\infty} \int_{-\infty}^{\infty} e^{-\frac{(u_m^2 + u_n^2 - 2\rho_{mn} u_m u_n)}{2} \frac{2(1-\rho_{mn}^2)}{\Delta}} \sin\left(\frac{2\pi k}{\Delta} u_m\right) \\ + \sin\left(\frac{2\pi \ell}{\Delta} u_n\right) \frac{du_m du_n}{2\pi\sigma\sqrt{1-\rho_{mn}^2}},$$

$$\sigma^2 \rho_{mn} = E(u_m u_n) = E(v_m v_n)$$

and

$$\rho_{mm} = \rho_{nn} = 1.$$

The above integral can be evaluated to yield finally

$$E\{e(u_m)e(u_n)\} \\ = \frac{\Delta^2}{\pi^2} \sum_{K, \ell=1}^{\infty} \frac{(-1)^{K+\ell}}{K\ell} e^{-2\pi^2 \left(\frac{\sigma}{\Delta}\right)^2 (K^2+\ell^2)} \sin\{4\pi^2 \left(\frac{\sigma}{\Delta}\right)^2 K\ell\rho_{mn}\} \quad (15)$$

Again for the cases of interest  $\Delta \ll \sigma$  so that to first order in

$e^{-2\pi^2 (\sigma/\Delta)^2}$  only the  $k=\ell$  terms need be kept. Thus

$$E\{e(u_m)e(u_n)\} = \frac{\Delta^2}{2\pi^2} \sum_{K=1}^{\infty} \frac{1}{K^2} e^{-4\pi^2 \left(\frac{\sigma}{\Delta}\right)^2 K^2 (1-\rho_{mn})} \quad (16) \\ + 0 \quad (e^{-2\pi^2 (\sigma/\Delta)^2})$$

Finally if  $\frac{\Delta^2}{12}$ , the quantization noise power, is set below the natural receiver noise of the radar, only the terms in (16) for which  $m=n$  will persist. To this final approximation

$$\begin{aligned} E e^2(u_n) &= \frac{\Delta^2}{2\pi^2} \sum_{k=1}^{\infty} \frac{1}{k^2} + o\left(e^{-2\pi^2 (\sigma/\Delta)^2}\right) \\ &= \frac{\Delta^2}{12} + o\left(e^{-2\pi^2 (\sigma/\Delta)^2}\right) \end{aligned} \quad (17)$$

and

$$E e(u_m) e(u_n) = 0 + o\left(e^{-2\pi^2 (\sigma/\Delta)^2 (1-\rho_{mn})}\right), \quad m \neq n,$$

using the well-known identity,

$$\sum_{k=1}^{\infty} \frac{1}{k^2} = \frac{\pi^2}{6}$$

If the quantization noise power is again set below the receiver noise, the imaginary part can be estimated in a similar manner to be

$$E e(u_n) e(v_n) = 0 + o\left(e^{-2\pi^2 (\sigma/\Delta)^2 (1-\mu_{nn})}\right) \quad (18)$$

for all  $m$  and  $n$  where

$$\sigma^2 \mu_{mn} = E u_m v_n = -E v_n u_m$$

In this case  $\mu_{mn} = 0$ , since by (7), (8) and (9),

$$B = EV^T = -EUV^T = -B^T$$

so that B is a skew symmetric matrix. Combining (17) and (18) yields

$$E \varepsilon(X) \{ \varepsilon(X) \}^* = \frac{\Delta^2}{6} I \quad (19)$$

where I is the N x N identity matrix as an estimate of the second term of (5), assuming the quantization noise is comparable to the receiver noise power.

A similar analysis will show (see reference 1) that the matrix elements of the third term of (5) are zero to the order of  $e^{-2\pi^2(\sigma/\Delta)^2}$ . Combining this with (19), yields finally,

$$M_Q = E[X][X]^* = M + \frac{\Delta^2}{6} I \quad (20)$$

to the order of  $e^{-2\pi^2(\sigma/\Delta)^2(1-\rho_{mn})}$ . This result will now be used to estimate losses in detection sensitivity an adaptive radar will suffer as a function of the quantization step  $\Delta$ . Better approximations to  $M_Q$ , then given by (20), particularly for a larger quantization step  $\Delta$ , will be the subject of a future study.

#### SIGNAL-TO-NOISE LOSS DUE TO QUANTIZATION

A best sampled-data filter of form (1) is one in which the weight vector W is chosen to maximize the signal-to-noise (S/N) ratio. The weight vector which achieves the optimum S/N ratio is well known (see

for example Reference 2) and given by

$$W_o = M^{-1}S \quad (21)$$

where  $M$  is the covariance matrix for noise only. Since  $M$  is often not known a priori, an estimate  $\hat{M}$  is used instead, depending on  $K$  samples of the noise process. One estimate is the sample average. If  $X^{(1)}, X^{(2)}, \dots, X^{(K)}$  are  $K$  independent samples of the noise process, then the sample average estimate of  $M$  is given by

$$\hat{M} = \frac{1}{K} \sum_{j=1}^K X^{(j)} X^{(j)*} \quad (22)$$

If  $\hat{M}$  is used in (21), then

$$\hat{W} = \hat{M}^{-1}S \quad (23)$$

is a near optimum set of weights to be used in filter (1). The output of this filter is

$$\hat{u} = \hat{W}^* X \quad (24)$$

where  $\hat{W}$  is given by (23). The output signal-to-noise ratio conditioned on a knowledge of  $\hat{W}$ , is

$$\begin{aligned} (S/N|_{\hat{W}})_o &= \frac{(Eu|_{\hat{w}})^2}{\text{Var}(\hat{u}|_{\hat{w}})} \\ &= (S \hat{M}^{-1} S)^2 / S \hat{M}^{-1} \hat{M} \hat{M}^{-1} S \end{aligned} \quad (25)$$

Previously it was shown [2] that if this signal-to-noise ratio was normalized with respect to its maximum value  $S^* M^{-1} S$  that this quantity, namely,

$$\rho(\hat{M}) = (S/N|\hat{w})_0 S^* M^{-1} S \quad (26)$$

was a random variable which was in the interval  $0 \leq \rho(\hat{M}) \leq 1$ . It was further found that this normalized signal-to-noise ratio has a probability density  $P(\rho)$  which depended only on  $N$ , the number of components of  $X$ , and the number  $K$  of sample vectors.

Previously in Reference 2 the quantity  $\rho(\hat{M})$  was the  $(S/N)$  loss ratio which depended on  $\hat{M}$ , the estimate of  $M$ , without any assumption of quantization. To make this ratio depend on quantization let  $\hat{M}_Q$  be the sample average estimate of  $M$ , including quantization, i.e. let

$$\hat{M}_Q = \frac{1}{K} \sum_{j=1}^K [X^{(j)}][X^{(j)}]^* \quad (27)$$

where  $[X^{(j)}]$  denotes the quantized value of sample vector  $X^{(j)}$ . Then the normalized signal-to-noise ratio for this estimate of  $M$  is

$$\begin{aligned} \rho_{\text{Total}}(\hat{M}_Q) &= \frac{(S/N|\hat{M}_Q)_0}{S^* \hat{M}_Q^{-1} S} \\ &= \frac{(S/N|M_Q)_0}{S^* \hat{M}_Q^{-1} S} \left( \frac{S^* M_Q^{-1} S}{S^* M^{-1} S} \right) \end{aligned}$$

$$= \rho(\hat{M}_Q) \left( \frac{S^* M_Q^{-1} S}{S^* M^{-1} S} \right) \quad (28)$$

where

$$M_Q = E[X][X]^*$$

is the complex covariance matrix of  $[X]$ , given by (5) and (20). For  $K$  reasonably large the statistics of  $[X]$  will be close to Gaussian, hence the statistics of  $\rho(\hat{M}_Q)$  will closely approximate the statistics of  $\rho(\hat{M})$  as given by (26). Thus, taking the expected value of (28), yields by equation (18) of Reference (2),

$$E\rho_{\text{Total}}(\hat{M}_Q) = \left( \frac{K+2-N}{K+1} \right) \left( \frac{S^* M_Q^{-1} S}{S^* M^{-1} S} \right) \quad (29)$$

This is the expected loss in S/N ratio, due firstly to the fact that only a finite number  $K$  of samples were used to estimate  $M$ , and secondly to the sample quantization. Expressed in decibels, this expected loss ratio is

$$\begin{aligned} \text{Loss} &= -10 \log_{10} \{ (K+2-N)/(K+1) \} \\ &\quad -10 \log_{10} \{ (S^* M_Q^{-1} S) / (S^* M^{-1} S) \} \end{aligned} \quad (30)$$

where the first term is the loss in decibels, due to the finite sampling in estimating  $M$ , and the second term is the loss due to quantization of finite step size  $\Delta$ . Using (20), an estimate of the last term can be

made from the identity,

$$\begin{aligned} M_Q^{-1} &= M^{-1}(I + \alpha M^{-1})^{-1} = M^{-1}(I - \alpha M^{-1}) + O(\alpha^2) \\ &\approx M^{-1} - \alpha M^{-2} \end{aligned}$$

where

$$\alpha = \Delta^2/6.$$

Hence

$$S^* M_Q^{-1} S = S^* M^{-1} S - \frac{\Delta^2}{6} S^* M^{-2} S$$

and

$$\begin{aligned} \text{Loss}_Q &= -10 \log_{10} \left( 1 - \frac{\Delta^2}{6} \frac{(S^* M^{-1} S)^2}{S^* M^{-1} S} \right) \\ &= -10 \log_{10} \left( 1 - \frac{\Delta^2}{6} \frac{W_0^* W_0}{S^* Y^{-1} S} \right) \end{aligned} \quad (31)$$

is the S/N loss due to quantization where  $W_0$  is the optimum weight vector (21). The reliability of these loss formulas will be checked by simulation during the next quarter.

REFERENCES

1. L. E. Brennan and I. S. Reed, "Quantization Noise in Digital Moving Target Indication Systems," IEEE Trans. on Aerospace and Electronic Systems, Vol. AE5-2, No. 6, Nov. 1966.
2. I. S. Reed, J. D. Mallett, L. E. Brennan, "Rapid Convergence Rate in Adaptive Arrays," IEEE Trans. of Aerospace & Electronic Systems, Vol. AES-10, No. 6, Nov. 1974.

APPENDIX II

FORTRAN PROGRAM FOR SIMULATION  
OF ADAPTIVE AMTI WITH NON-LINEARITIES

## PROGRAM ADAPTM8

```

C
C MOD INCLUDES SAMPLE MATRIX INVERSION SMI, INVERSE MATRIX UPDATE
C IMU, AND APPLEBAUM LOOPS
C NP=NUMBER OF PULSES
C NEL=NUMBER OF ANTENNA ARRAY ELEMENTS
C NSC=NUMBER OF CLUTTER SCATTERERS PER RANGE RING
C ALL DISTANCES ARE MEASURED IN WAVELENGTHS
C D=DISTANCE RADAR PLATFORM MOVES BETWEEN PULSES
C ELSPAC=ELEMENT SPACING
C THETAD=INITIAL SCAN ANGLE IN DEGREES, MEASURED FROM GROUND TRACK
C THDOTD=SCAN RATE IN DEGREES PER PULSE REPETITION PERIOD
C RECNR=RATIO OF RECEIVER NOISE TO CLUTTER POWERS
C SIG=AMPLITUDE OF STEERING SIGNALS IN LOOPS
C XR=ANY RANDOM NUMBER TO INITIALIZE THE CLUTTER AND NOISE GENERATORS
C IELPAT CONTROLS THE ELEMENT PATTERN***IELPAT=1 FOR APS/96 ELEMENT PA
C OTHERWISE THE ELEMENT PATTERN IS ISOTROPIC
C IEIG=1 NORMAL COORDINATES USED IN SIMULATION
C NPR=SAMPLES IN ONE GROUP
C NBP=NUMBER OF GROUPS
C AL=WEIGHTING OF NEW DATA FOR IMU
C DLSG = DEL/SG
C ITL SELECTS CASE NSC1 VALUES OF DLSG OR BITS
C NSC2 VALUES OF AK (AK * SG = SAT)
C ITL = 0 LIMITING ONLY NSC1=1, DLSG=0, NSC2 VALUES OF AK
C ITL = 1 QUANT ONLY NSC1 VALUES OF DLSG, NSC2=1, AK .GE. 5
C ITL = 3 QUANT AND LIMITING NSC1 VALUES OF NUMBER OF HITS AND NSC2
C VALUES OF AK FOR EACH ABIT VALUE

CALL MAIN
STOP
END

```

## SUBROUTINE MAIN

```

COMPLEX W(30), WD(30), SCAT(60), SST(30), DCT(30)
COMPLEX GAIN(30,60), VS(8,320), SC(30,30), CM(30,30), V(8,320)
COMPLEX CN(30,30), A(30,30), B(30,30), CO(30,30), CC, SS
REAL LSS, LTOT
DIMENSION EIG(30), SEIG(30), CAS1(20), CAS2(20)
DIMENSION Y11(500), Y12(500), Y21(500), Y22(500), Y31(500), Y32(500)
DIMENSION X1(500), SCL(500), X2(100), SCS(100), X3(100), SCI(100)
COMMON/PARAM/NP, NEL, NPL, NSC, SIG
COMMON/ARRAY/GAIN, VS, SST
COMMON/B/W, WD
COMMON/M/SC
COMMON/N/CM
COMMON/P/X1, X2, X3, SCL, SCS, SCI, I1, I2, I3, INV, LP, ISP, NRS
COMMON/Q/CO
COMMON/R/DCT, THDCT, ADCT, JDCT
COMMON/NS/ICX, ICY, ICT
COMMON/Y/Y11, Y12, Y21, Y22, Y31, Y32
NAMELIST/INPUT/ NP, NEL, NSC, NRUNG, NSIC, NPR, INV, LP, ISP, NRS,

```

```

1ERR,GLOP,AL,NBP,D,8IG,XR,IELPAT,ELSPAC,THETAD,THDOTD,RECN,
2IEIG,IPL0T,ASIG,ADCT,THDCTD,JDCT,KDCT,AK,NBIT,DEL,SAT,DL5G
3,TLDB,NRNS,NCS1,NCS2,ITL,ILT
  READ(5,INPUT)
  IF(NEL,EQ,0) RETURN
  ISAV=IEIG
  PI=4.*ATAN(1.)
  RAD=PI/180.
  XR=RANF(XR)
  NRUNS=NBP*NPR
1  FORMAT(10F5.1)
  THDOT=THDOTD*RAD
  THETA=THETAD*RAD
  THDCT=THDCTD*RAD
  NPL=NP*NEL
  WRITE(6,INPUT)
C  IDEAL PERFORMANCE AT ANGLE THETA
  NR=1
  CALL P,ASE (D,CONST,SCZERO,IELPAT,ELSPAC,THETA,THDOT,0,NR)
  WRITE(6,542) CONST,SCZERO
  SRECN=RECN*NEL**3/2./SCZERO*SIG**2
  VRECN=SQRT(SRECN)
C  IDEAL COV. MATRIX
  CALL CVM(NPL,SC,NSC,SRECN)
  TAU=GLOP*REAL(CM(1,1))*NPL/2./ERR
  PRINT 500,TAU
  PRINT 500,(SC(I,I) ,I=1,NPL)
  CC=0.
12 DO 12 I=1,NPL
  CC=CC+SC(I,I)
  CC=CC/NPL/2.
  SG=SQRT(CABS(CC))
  PRINT 530,SG
  PRINT 510
  PRINT 502
  CALL WTS(W,SC,CONST,0,0)
C  SC = INVERSE IDEAL MATRIX
  NRS=4S I3=1
  CALL SIGCN(W,SST,NPL,CONST)
  NRS=3
  CALL SIGCN(W,SST,NPL,CONST)
  S1=SCI(1)
  SCI(1)=10.*ALOG10(SCI(1))
  SSG=SCI(1)
  SCS(1)=SSG
C  DIAGONAL OF SC
  PRINT 510
  PRINT 500,(SC(I,I),I=1,NPL)
C  COMP VS FOR EACH SAMPLE
  AD=ADCT*NPR*NBP
  NBPR = NPR*NBP
  DO 31 J = 1,NBPR

```

```

CALL SCGEN(NSC,SCAT,XR)
DO 31 L=1,NPL
CC=0.
IF(J,EQ,NSIC) CC = ASIG*CONJG(SST(L))
IF(J,EQ,JDCT) CC = CC+AD*DCT(L)
DO 32 K=1,NSC
CC=CC+SCAT(K)*GAIN(L,K)
32 CONTINUE
31 VS(L,J)=CC
IF(RECN,GT,0.) CALL NADD(J,NBPR,VRECN,XR)
DO 37 J=1,NBPR
DO 37 L=1,NPL
37 V(L,J)=VS(L,J)
CST=0.
DO 20 J=1,NBPR
DO 20 L=1,NPL
20 CST=CST+REAL(V(L,J)*CONJG(V(L,J)))
CST=CST/2.
SG=SQRT(CST/(NBPR*NPL))
PRINT 530,SG
SS = 0.
CC = 0.
DO 10 I = 1,NPL
SS = SS+W(I)*CONJG(W(I))
10 CC = CC+SST(I)*CONJG(W(I))
AC=REAL(CC/SS)
XX=SI/CONST
PRINT 500,AC,XX

C
C
C
16 CONTINUE
NBPR=NPR*NBP
LSS=10.*ALOG10((NPR+2.*NPL)/(NPR+1.))
NB=NBP+1
DO 94 I=1,NB
94 SCI(I)=SSG
PRINT 509,ITL,ILT
READ(5,1) (CAS1(I),I=1,NCS1)
READ(5,1) (CAS2(I),I=1,NC82)
DO 301 IS=1,NCS1
DLSG=CAS1(IS)
DO 300 IR=1,NC82
ICX=ICY=ICT=0
PRINT 510
PRINT 510
PRINT 500,CAS1(IS),CAS2(IR)
AK=CAS2(IR)
DO 35 M = 1,NPL
DO 35 N = 1,NBPR
35 VS(M,N) = V(M,N)
IF(ITL,EQ,0) GO TO 22

```

```

IF(ITL, EQ, 1) GO TO 4
IF(ITL, EQ, 3) GO TO 3
TLDB=CAS1(IS)
TLOS=10, **(-CAS1(IS)/10,)
DLSG=SQRT((1,-TLOS)*AC*6,)/SG
4 CONTINUE
IF(DLSG, LE, 0,) GO TO 91
NL=2,*AK /DLSG+.5
NBIT=ALOG(NL+2,)/ALOG(2,)+.5
AK=DLSG*NL/2,
GO TO 5
3 NBIT=CAS1(IS)+.5
NL=2**NBIT-2
DLSG=2,*AK/NL
5 CONTINUE
DS1=(DLSG*SG)**2/6,
DO 14 M=1,NPL
DO 14 N=1,NPL
CC =CM(M,N)
IF(M, EQ, N) CC=CC +DS1
14 SC(M,N)=CC
CALL MATINV(NPL, SC)
CC=0,
DO 11 M=1,NPL
SS=0,
DO 13 N=1,NPL
13 SS=SS+SC(M,N)*SST(N)
11 CC=CC+CONJG(SST(M))*SS
SSC=REAL(CC)*CONST
XX=SSC
TLD1=10,*ALOG10(SSC)-SC1(1)
LTOT=LSS+TLD1
PRINT 525, TLD1, LSS, LTOT
XX=1,-DS1/AC
IF(XX, GT, 0,) DB = 10,*ALOG10(ABS(XX))
PRINT 500, XX, DB
ABIT=NBIT
ANL=NL
22 CONTINUE
SAT=SG*AK
PRINT 526
PRINT 500, SAT, AK, TLDB, DLSG, ABIT, AC, CC, SS, ANL
IF(ILT, EQ, 1) CALL QUANT1(VS, NL, SAT, NPL, NBPR, ITL)
IF(ILT, EQ, 2) CALL QUANT2(VS, NL, SAT, NPL, NBPR, ITL)
CT=FLOAT(ICT)
CX=FLOAT(ICX)
CY=FLOAT(ICY)
PRINT 514
PC=(CX+CY)/CT*100,
PRINT 516, PC
PRINT 500, CT, CX, CY
PRINT 510

```

```

91  CONTINUE
    I1=1$I2=1$I3=1
    X1(1)=0$X2(1)=0$X3(1)=0
    NPL4=4*NPL
C
C  BIG LOOP
C  SIMULATION USING RANDOM CLUTTER SAMPLES
    NBO=1
    NCT=0
    JJ=0
    DO 87 I = 1,NBP
      JJ = JJ+NPR
C
C  8MI
    NR=2
    I2=I2+1
    X2(I2)=JJ
    N1=JJ+NPR+1
    CALL SAMPLE(NPL,NPR,I,CONST,N1)
    2  CONTINUE
    87  CONTINUE
C
    AV = 0.
    AVS=0.
    VA = 0.
    IZ=I2+1
    DO 28 I = 2, IZ
      AVS=AVS+SCS(I)
    28 AV = AV+SCI(I)
      AV=AV/(NBP-1)
      AVB=AVS/(NBP-1)
      VA=0.$VAS=0.
      DO 29 I = 2, IZ
        IF(I,EQ,I3) GO TO 90
        VAS=VAS+(SCS(I)/AVS-1.)*2
        VA =VA +(SCI(I)/AV -1.)*2
    90 SCS(I)=10.*ALOG10(SCS(I))
    29 SCI(I)=10.*ALOG10(SCI(I))
      VA=VA/(NBP-1)
      VAS=VAS/(NBP-1)
      AV =10.*ALOG10(AV )=SCI(1)
      AVS=10.*ALOG10(AVB)=SCI(1)
      PRINT 504
      PRINT 500,(X2(I),I=1,I2)
      PRINT 506
      PRINT 515,AVS,VAS
      PRINT 500,(SCS(I),I=1,I2)
      AVL=0.
      VAL=0.

```

```

DO 30 I=3,12
30  AVL=AVL+SCL(I)
   AVL=AVL/(NBP-1)
   DO 36 I=3,12
   VAL=VAL+(SCL(I)/AVL-1)**2
36  SCL(I)=10.*ALOG10(SCL(I))
   VAL=VAL/(NBP-1)
   AVL=10.*ALOG10(AVL)=SCI(I)
   PRINT 515,AVL,VAL
   PRINT 500,(SCL(I),I=3,12)
   PRINT 510
   IF(INV,EQ,1)
1  PRINT 507
   IF(INV,EQ,1)
2  PRINT 500,AV,VA
   IF(INV,EQ,1)
3  PRINT 500,(SCI(I),I=1,I3)
   PRINT 510
   GO TO (80,81,82), IS
80  Y11(IR)=SSG+AV8
   Y12(IR)=SSG+AVL
   GO TO 300
81  Y21(IR)=SSG+AV8
   Y22(IR)=SSG+AVL
   GO TO 300
82  Y31(IR)=SSG+AV8
   Y32(IR)=SSG+AVL
300 CONTINUE
301 CONTINUE
   DO 302 I = 1,NCS2
302  X1(I)=CAS2(I)
   IF(IPLOT,EQ,1) CALL BPLOT(NCS2,SSG)
   XR=RANF(-1.)
   AK=AKS
   READ INPUT
   IF(NEL,EQ,0) RETURN
   XR=RANF(XR)
   GO TO 16
500  FORMAT(1X,8E16.7)
501  FORMAT(/,* NUMBER OF SAMPLES = *,I5)
502  FORMAT(/,* OPT PERFORMANCE*)
503  FORMAT(/,* XR* *,F17.10,* TAU* *,E17.10)
504  FORMAT(* X AXIS*)
506  FORMAT(* SAMPLE MATRIX INVERSION(SMI,SCS)*)
507  FORMAT(* INVERSE MATRIX UPDATE(IMV,SCI)*)
508  FORMAT(1X,10I4)
509  FORMAT(/,* ITL= *,I4,* ILT= *,I4)
510  FORMAT(/)
511  FORMAT(/,* EIGEN VALUES*)
512  FORMAT(/,* IDEAL COVAR. MATRIX*)
513  FORMAT(/,* NORMAL MATRIX*)
514  FORMAT(1X,* CYOT CX CY*)

```

```

515 FORMAT(/,IX,*SIMULATION LOSS = *,F10.3,*VARIANCE = *,F10.3)
516 FORMAT(/,IX,*PERCENT LIMITING = *,F10.3)
525 FORMAT(/,IX,*TH, QUANT LOSS DB = *,F10.3,*TH, SAMPLE LOSS = *,F10.
13,*TOTAL TH, LOSS = *,F10.3)
526 FORMAT(/,* SAT AK TLDB DLSG ABIT AC CC SS*)
527 FORMAT(IX,10,F12.3)
530 FORMAT(/,* SG= *,2E16.7)
542 FORMAT(7H CONST*,E16.6,10X,7HSCZERO=E16.6//)
END

```

```

SUBROUTINE B PLOT(NSP,SSG)
COMMON /PARAM/ NP,NEL,NPL,NSC,SIG
DIMENSION Y11(500),Y12(500),Y21(500),Y22(500),Y31(500),Y32(500)
DIMENSION X1(500),SCL(500),X2(100),SCS(100),X3(100),SCI(100)
DIMENSION AM(500)
COMMON/P/X1,X2,X3,SCL,SCS,SC1,I1,I2,I3,INV,LP,ISP,NRS
COMMON/Y/Y11,Y12,Y21,Y22,Y31,Y32
DO 3 I = 1,NSP
3 AM(I) = SSG
NS1=NSP+1
NS2=NSP+2
X1(NS1)=2.
X1(NS2)=1.0
Y11(NS1)=10.
Y12(NS1)=10.
Y21(NS1)=10.
Y22(NS1)=10.
Y31(NS1)=10.
Y32(NS1)=10.
Y11(NS2)=5.
Y12(NS2)=5.
Y21(NS2)=5.
Y22(NS2)=5.
Y31(NS2)=5.
Y32(NS2)=5.
AM(NS1)=10.
AM(NS2)=5.
CALL PLOT1SC(7HMALLET,1.)
CALL AXIS(0.,0.,,7HSAT/SIG,,7.6,,0.,2.,,1.0,0)
CALL AXIS(0.,0.,,12HMT1 GAIN(DB),,12.8,,90.,,10.,,5.,,=1)
HT=(SSG-Y32(NS1))/Y32(NS2)+0.1
CALL SYMBOL(3,0,HT,,1,23HSTEADY STATE GAIN(DB) =,0.,23)
CALL NUMBER(5,0,HT,,1,SSG,0.,,4HF6.1)
CALL LINE(X1,AM,NSP,1,0,0)
CALL LINE(X1,Y11,NSP,1,1,1)
CALL LINE(X1,Y12,NSP,1,1,2)
CALL LINE(X1,Y21,NSP,1,1,1)
CALL LINE(X1,Y22,NSP,1,1,2)
CALL LINE(X1,Y31,NSP,1,1,1)
CALL LINE(X1,Y32,NSP,1,1,2)
CALL PLOT(10.,0.,,=3)

```

RETURN  
END

```

C SUBROUTINE PHASE(D,CONST,SCZERO,IELPAT,ELSPAC,THETA ,THDOT ,NC,NR)
  COMPUTES RETURN FROM EACH SCATTER TO EACH ELEMENT
  COMMON/PARAM/NP,NEL,NPL,NSC,SIG
  COMMON/ARRAY/GAIN,VS,SST
  COMMON/R/DCT,THDCT,ADCT,JDCT
  COMPLEX GAIN(30,60),VS(8,320),DCT(30),SST(30),CP
  PI=4.*ATAN(1.)
  CP=CMPLX(0.,2.*PI)
  CZERO=0.
  THMIN=THETA-PI/2.
  THMAX=THETA+PI/2.
  C=(THMAX-THMIN)/NSC
  KK=INT((THDCT-THMIN)/C+1)
  THDCT=THMIN+(KK-.5)*C
  NS=NSC+INT((NR*THDOT)/C)+1
  PSI=THETA+NC*THDOT
  DO 10 K=1,NS
    TH=THMIN+(K-.5)*C
    CC=COS(TH)
    DO 10 M=1,NP
      MNM=M+1+NC
      SS=PSI-TH
      IF (ABS(SS).GT,PI/2.) GO TO 10
      SS=SIN(SS)
      GT=NEL
      IF (SS.EQ,0) GO TO 88
      GT=SIN(PI*ELSPAC*SS*NEL)/SIN(PI*ELSPAC*SS)
88 CONTINUE
      IF (IELPAT.NE,1) GO TO 30
      GAM=.207*COS(PSI-TH)*.238
      ELP=SIN(21.*PI*GAM)/SIN(PI*GAM)
      GT=GT*ELP**2
30 CONTINUE
      IF (M.EQ,1) CZERO=CZERO+ GT**4
      DO 10 N=1,NEL
        L=(M+1)*NEL+N
        GAIN(L ,K)=GT*CEXP(=CP*((N-(NEL+1))/2.)*SS*ELSPAC*MNM *2,*D*CC))
        IF (K.EQ,KK) DCT(L)=GAIN(L,K)
10 CONTINUE
      SCZERO=NEL**4*SIG**2/CZERO
      CONST=NEL**2/SCZERO
      IF (JDCT.EQ,0) GO TO 31
      CC=COS(THDCT)
      SS=PSI-THDCT
      GT=0.
      IF (ABS(SS).GT,PI/2.) GO TO 91
      SS=SIN(SS)
      GT=NEL

```

```

IF(SS, EQ, 0) GO TO 91
GT=SIN(PI*ELSPAC*SS*NEL)/SIN(PI*ELSPAC*SS)
91 CONTINUE
IF(IELPAT, NE, 1) GO TO 31
TH=THDCT
GAM=.207*COS(PSI-TH)*.238
ELP=SIN(21,*PI*GAM)/SIN(PI*GAM)
GT=GT*ELP**2
31 CONTINUE
DO 20 M=1, NP
L=(M-1)*NEL+1
MNM=NC+M-2
SST(L )=SIG*CEXP(=CP*( MNM*2,*D*COS(PSI ) +(M-1)/2.))
DO 20 N=1, NEL
LL=L+N
IF(JDCT, EQ, 0) GO TO 92
I=L+N-1
DCT(I)= GT*CEXP(=CP*((N-(NEL+1))/2.)*SS*ELSPAC=MNM *2,*D*CC))
92 CONTINUE
20 SST(LL )=SST(L)
RETURN
END

```

```

SUBROUTINE NADD(J, NPR, RECN, XR)
C REC, NOISE GEN.
COMPLEX SST(30), GAIN(30, 60), VS(8, 320), CP
COMMON/PARAM/NP, NEL, NPL, NSC, SIG
COMMON/ARRAY/GAIN, VS, SST
CP=CMPLX(0., 2.*3.14159265)
DO 10 J=1, NPR
DO 10 M=1, NPL
XR=RANF(0.)
AMP=RECN*SQRT(= ALOG(XR))
XR=RANF(0.)
10 VS(M, J)=VS(M, J)+AMP*CEXP(CP*XR)
RETURN
END

```

```

SUBROUTINE WTS(W, CM, CONST, J1, J2)
C OPTIMUM WEIGHTS
COMPLEX SST(30), W(30), CFPREC, C, S
COMPLEX CM(30, 30), GAIN(30, 60), VS(8, 320)
COMMON/PARAM/NP, NEL, NPL, NSC, SIG
COMMON/ARRAY/GAIN, VS, SST
S=0.
NMAT=NP*NEL
IF(J1, EQ, 1) CALL MATINV(NMAT, CM)
IF(J2, NE, 2) PRINT 91
91 FORMAT(/7X, 6HPULSE , 4X, 7HELEMENT, 6X, 4HREAL, 5X, 9HIMAGINARY, 5X,
19HAMPLITUDE, 5X, 5HPHASE//)

```

```

DD 90 M=1,NP
J=(M-1)*NEL
DD 90 N=1,NEL
MM=N+J
C=0,
DO 31 M1=1,NP
I=(M1-1)*NEL
DO 31 N1=1,NEL
NN=N1+I
C=C+SST(NN)*CM(MM,NN)
31 CONTINUE
S=S+C*CONJG(SST(MM))
W(MM)=C
IF(J2.EQ,2) GO TO 90
AMP=CABS(C)
PHA=ATAN2(AIMAG(C),REAL(C))
WRITE(6,50) M,N,C,AMP,PHA
90 CONTINUE
IF(J2.NE,0) RETURN
50 FORMAT(2I11,5X,2F20,9,2F12,7)
SR=CABS(S)
IF(SR.LT,10,E=10) GO TO 2
SSR=SR
SR=10,*ALOG10(SR)
CST=10,*ALOG10(CONST)
GO TO 3
2 CONTINUE
SRX=0,
3 SRX=SR+CST
PRINT 52,SR,SRX
52 FORMAT(/5X,7HWS(DB)=,G15,8,14HS/C*CONST(DB)=,G15,8)
RETURN
END

```

```

SUBROUTINE SCGEN(NSC,SCAT,XR)
C NOISE GEN. FOR EACH SCATTERER
CO PLEX CP,SCAT(60)
CP=CMPLX(0.,2.*3.14159265)
DO 10 N=1,NSC
AMP=RANF(0.)
XR=RANF(0.)
10 SCAT(N)=SQRT(-ALOG(AMP))*CEXP(CP*XR)
RETURN
END

```

```

SUBROUTINE SIGCN(W,SST,NPL,CONST)
C COMPUTE SIG/ CLUT USING WTS ON IDEAL MATRIX
COMMON/N/CM
COMMON/P/X1,X2,X3,SCL,SCS,SCI,I1,I2,I3,INV,LP,ISP,NRS
DIMENSIONX1(500),SCL(500),X2(100),SCS(100),X3(100),SCI(100)

```

```

COMPLEX CM(30,30),W(30),SST(30),CC,SS,CB
SS=0.
CC=0.
DO 71 M=1,NPL
SS=SS+W(M)*CONJG(SST(M))
CB=0.
DO 70 N=1,NPL
70 CB=CB+      W(N)*CM(M,N)
71 CC=CC+CB*CONJG(W(M))
SSR=CABS(SS)**2
CCR=CABS(CC)
SCD=SSR/CCR*CONST
SCR=SCD
IF(NRS,EQ,1) SCL(I1)*SCR
IF(NRS,EQ,3) SCI(I3)=SCR
IF(NRS,EQ,2) SCS(I2)=SCR
IF(NRS,NE,4) GO TO 2
SCDB=10.*ALOG10(SCD)
SSR=10.*ALOG10(SSR)
CCR=10.*ALOG10(CCR)
WRITE(6,80) SSR,CCR,SCDB
80 FORMAT(/8H SIGNAL=,F10.5,4X,14HCLUTTER POWER=,F10.5,4X,8HS/C(DB)
1,F10.5)
2 CONTINUE
RETURN
END

```

```

C SUBROUTINE CVM(NPL,SC,NSC,SRECN)
FORMS STEADY STATE COV, MATRIX
COMPLEX SST(30),DCT(30),CC
COMPLEX CM(30,30),SC(30,30),GAIN(30,60),VS(8,320)
COMMON/ARRAY/GAIN,VS,SST
COMMON/N/CM
COMMON/R/DCT,THDCT,ADCT,JDCT
A=ADCT*ADCT
DO 10 M=1,NPL
DO 10 N=M,NPL
CC=0.
IF(JDCT,NE,0) CC=CC+A*DCT(N)*CONJG(DCT(M))
DO 21 J=1,NSC
21 CC=CC+GAIN(N,J)*CONJG(GAIN(M,J))
IF(M,EQ,N) CC=CC+SRECN
CM(M,N)=CC*SC(M,N)=CONJG(CC)
SC(M,N)=CC*SSC(N,M)=CONJG(CC)
10 CONTINUE
RETURN
END

```

```

SUBROUTINE SAMPLE(NPL,NPR,I,CONST,N1)
COMPLEX W(30),WO(30),SST(30),CC

```

```

COMPLEX CU(30,30),CN(30,30),CZ(30,30),GAIN(30,60),VS(8,30)
COMMON/Q/CD
COMMON/B/W,W0
COMMON/ARRAY/GAIN,VS,SST
C COMPUTE SAMPLE COV. MATRIX

```

```

N2=N1+NPR-1
A=1./I
IF(I.NE.1) GO TO 2
A=1.
DO 8 M=1,NPL
DO 8 N=1,NPL
8 CN(M,N)=0.
2 CONTINUE
IF(A.GT.1.) A=1.
DO 11 M=1,NPL
DO 11 N=M,NPL
CC=0.
DO 30 K=N1,N2
30 CC=CC+CONJG(VS(M,K))*VS(N,K)
CONTINUE
CN(M,N)=CC/NPR
CZ(M,N)=CN(M,N)
CN(N,M)=CONJG(CN(M,N))
CZ(N,M)=CN(N,M)
11 CONTINUE
501 FORMAT(1X,* SAMPLE INVERSION*)
CALL WTS(W,CN,CONST,0,2)
CALL SIGC2(W,SST,NPL,CONST,1,CZ)
3 CONTINUE
RETURN
END

```

```

SUBROUTINE SIGC2(W,SST,NPL,CONST,I,UM)
COMMON/P/X1,X2,X3,SCL,SCS,SCI,I1,I2,I3,INV,LP,ISP,NRS
DIMENSIONX1(500),SCL(500),X2(100),SCS(100),X3(100),SCI(100)
COMPLEX UM(30,30),W(30),SST(30),CC,SS,CB,US(30,30)
SS=0.
CC=0.
DO 71 M=1,NPL
SS=SS+W(M)*CONJG(SST(M))
CB=0.
DO 70 N=1,NPL
70 CB=CB+W(N)*UM(M,N)
71 CC=CC+CB*CONJG(W(M))
SSR=CAHS(SS)**2
CCR=CAHS(CC)
SCN=SSR/CLP*CONST
SCS(I2)=SCL
IF(I.EQ.1) GO TO 5

```

```

      CC=0,
      DO 1 M=1,NPL
      CB=0,
      DO 2 N=1,NPL
2     CB=CB+          W(N)*US(M,N)
1     CC=CC+CONJG( W(M))*CB
      CCR=CABS(CC)
      SCL(I2)=SSR/CCR*CONST
5     CONTINUE
      DO 6 M=1,NPL
      DO 6 N=1,NPL
6     US(M,N)=UM(M,N)
      RETURN
      END

```

```

C     SUBROUTINE QUANT1(V,NL,SAT,NPL,NPR,ITL)
      QUANTIZATION SUBROUTINE FOR A/D CONVERTER OF FIGURE 3
      COMPLEX V(8,320)
      COMMON/NS/ICX,ICY,ICT
      DO 10 M = 1,NPL
      DO 10 N = 1,NPR
      ICT=ICT+1
      XX=REAL(V(M,N))
      XA=ABS(XX)
      YY=AIMAG(V(M,N))
      YA=ABS(YY)
      IF(XA,LT,SAT) GO TO 9
      XX=SAT*XX/XA
      ICX=ICX+1
9     IF(YA,LT,SAT) GO TO 5
      YY=SAT*YY/YA
      ICY=ICY+1
5     IF(ITL,EQ,0) GO TO 10
      ZX = (XX/2./SAT + .5)*(NL )+.5
      ZY = (YY/2./SAT + .5)*(NL )+.5
      XX = AINT(ZX)/(NL )*2*SAT-SAT
      YY = AINT(ZY)/(NL )*2*SAT-SAT
10    V(M,N)=CMPLX(XX,YY)
      RETURN
      END

```

```

C     SUBROUTINE QUANT2(V,NL,SAT,NPL,NPR,ITL)
      QUANTIZATION SUBROUTINE FOR A/D CONVERTER OF FIGURE 3
      COMPLEX V(8,320)
      COMMON/NS/ICX,ICY,ICT
      DO 10 M = 1,NPL
      DO 10 N = 1,NPR
      AMP=CABS(V(M,N))
      ICT=ICT+1
      IF(AMP,LT,SAT) GO TO 5

```

```

V(M,N)=V(M,N)*SAT/AMP
ICX=ICX+1
5 IF(ITL,EQ,0) GO TO 10
XX=REAL(V(M,N))
YY=AIMAG(V(M,N))
ZX = (XX/2./SAT + .5)*(NL )+.5
ZY = (YY/2./SAT + .5)*(NL )+.5
XX = AINT(ZX)/(NL )*2*SAT-SAT
YY = AINT(ZY)/(NL )*2*SAT-SAT
10 V(M,N)=CMPLX(XX,YY)
RETURN
END

```

```

SUBROUTINE MATINV(N,A)
COMPLEX A(30,30)
DO 11 N1=1,N
DO 12 J=1,N
IF(J,EQ,N1) GO TO 12
A(N1,J)=A(N1,J)/A(N1,N1)
12 CONTINUE
DO 15 I=1,N
IF(I,EQ,N1) GO TO 15
DO 16 J=1,N
IF(J,EQ,N1) GO TO 16
A(I,J)=A(I,J)-A(I,N1)*A(N1,J)
16 CONTINUE
A(I,N1)=-A(I,N1)/A(N1,N1)
15 CONTINUE
A(N1,N1)=1./A(N1,N1)
11 CONTINUE
RETURN
END

```

DISTRIBUTION LIST

Commander  
Naval Air Systems Command  
Department of the Navy  
Washington, D. C. 20361  
Attn: AIR-533D3 (1 copy quarterly) (3 copies final)  
AIR-50174 (14 copies final only)  
AIR-310B (2 copies quarterly) (5 copies final)

Commander  
Naval Sea System Command  
Department of the Navy  
Washington, D. C. 20360  
Attn: SEA-034

Commander  
Department of the Air Force  
Air Force Avionics Laboratory  
Electronic Warfare Division  
Wright-Patterson Air Force Base  
Ohio 45433  
Attn: Mr. Harold Weber

Commanding Officer  
Naval Air Development Center  
Warminster, Pennsylvania 18974  
Attn: Mr. Jerry Guarini, AER-2

Director  
Naval Research Laboratory  
Washington, D. C. 20390  
Attn: Mr. Fred Staudaher, Code 5368 (1 copy)  
Mr. D. Stilwell, Code 7945 (1 copy)

Commander  
Naval Weapons Center  
China Lake, California 93555  
Attn: Code 35  
Code 40  
Code 601

Commanding Officer  
Naval Avionics Facility  
Indianapolis, Indiana 46218  
Attn: Mr. Paul Brink

Commander  
Naval Electronics Laboratory Center  
San Diego, California 92152  
Attn: Code 2330 (2 copies)

General Dynamics/Electronics Division  
P. O. Box 81127  
San Diego, California 92138  
Attn: Dr. G. Tricoles

Director  
Electro-Sciences Laboratory  
Ohio State University  
1320 Kinnear Road  
Columbus, Ohio 43212  
Attn: Mr. Robert Fouty

Commander  
Air Force Cambridge Research Laboratory  
Laurence C. Hanscom Field  
Bedford, Massachusetts 01730  
Attn: Mr. Philip Blacksmith

Harry Diamond Laboratories  
Microwave Research and Development Branch  
Connecticut Avenue and Van Ness Street, N. W.  
Washington, D. C. 20438  
Attn: Mr. Howard S. Jones, Jr.

Syracuse University Research Corporation  
Merrill Lane  
University Heights  
Syracuse, New York 13210  
Attn: Mr. Sidney Applebaum

Dr. Norbert N. Bojarski  
16 Circle Drive  
Moorestown, New Jersey 08057

Hughes Aircraft Company  
Radar Microwave Laboratory  
Cantinella and Teale  
Culver City, California 90230  
Attn: Dr. W. Kummer

Polytechnic Institute of New York  
Department of Electrical Engineering and Electrophysics  
Farmingdale, New York 11735  
Attn: Dr. Alexander Hessel

Tennessee Technological University  
College of Engineering  
Cookeville, Tennessee 38501  
Attn: Dr. Roy Adams

R. C. Hansen, Inc.  
Suite 218  
17100 Ventura Blvd.  
Encino, California 91316

Naval Ammunition Depot  
Crane, Indiana 47448  
Attn: Mr. Rod C. Davis, Code 3083